Elucidation of the Controlled Release Behavior of Metoprolol Succinate from Directly Compressed Xanthan Gum-Chitosan Polymers: Computational and Experimental Studies

Suha M. Dadou, Musa I. El-Barghouthi, Milan D. Antonijevic, Babur Z. Chowdhry, and Adnan A. Badwan

Elucidation of the Controlled Release Behavior of Metoprolol Succinate from Directly Compressed Xanthan Gum-Chitosan Polymers: Computational and Experimental Studies

Suha M. Dadou[a], Musa I. El-Barghouthi[b, c], Milan D. Antonijevic[a],

Babur Z. Chowdhry[a], Adnan A. Badwan[d*]

[a] *Department of Pharmaceutical, Chemical & Environmental Science, Faculty of Engineering & Science, University of Greenwich, Medway Campus, Chatham Maritime, Kent ME4 4TB, UK;*

[b] *Department of Chemistry, The Hashemite University, P.O. Box 150459, Zarqa 13115, Jordan;*

[c] *Department of Chemistry, Isra University, Amman 11622, Jordan;*

[d] *Research and Innovation Centre, The Jordanian Pharmaceutical Manufacturing Company (PLC), P.O. Box 94, Naor 11710, Jordan.*

Corresponding author's e-mail: dr.badwan@jpm.com.jo

ABSTRACT

The development and evaluation of a controlled-release (CR) pharmaceutical solid dosage form comprising xanthan gum (XG), low molecular weight chitosan (LCS) and metoprolol succinate (MS) is reported. The research is, partly, based upon the utilization of computational tools; in this case molecular dynamics simulations (MDs) and response surface method (RSM), in order to underpin the design/prediction and to minimize the experimental work required to achieve the desired pharmaceutical outcomes. The capability of the system to control the release of MS was studied as a function of LCS (% w/w) and total polymer (LCS and XG) to drug ratio (P:D) at different tablet tensile strengths. MDs trajectories, obtained by using different ratios of XG:LCS as well as XG and high molecular weight CS (HCS), showed that the driving force

for the interaction between XG and LCS is electrostatic in nature, the most favourable complex is formed when LCS is used at 15 % (w/w) and, importantly, that the interaction between XG and LCS is more favourable than that between XG and HCS. RSM outputs revealed that the release of the drug from the LCS/XG matrix is highly dependent on both the % LCS and the P:D ratio and that the required CR effect can be achieved when using weight fractions of LCS ≤ 20% and P:D ratios ≥ 2.6:1. Results obtained from in-vitro drug release and swelling studies on the prepared tablets showed that using LCS at the weight fractions suggested by MDs and RSM data plays a major role in overcoming the high sensitivity of the controlled drug release effect of XG on ionic strength and pH changes of the dissolution media. In addition, it was found that polymer relaxation is the major contributor to the release of MS from LCS-XG tablets. Using Raman spectroscopy, MS was shown to be localized more in the core of the tablets at the initial stages of dissolution due to film formation between LCS and XG on the tablet surface which prevents excess water penetration into the matrix. In the later stages of the dissolution process, the film starts to dissolve/erode allowing full tablet hydration and a uniform drug distribution in the swollen tablet.

Keywords: Low molecular weight chitosan, xanthan gum, molecular dynamics simulations, response surface method, controlled-release polymeric matrices, pharmaceutical formulation, tablet swelling, Raman mapping, metoprolol succinate.

Introduction

Oral controlled release (CR) drug delivery systems are generally manufactured by utilizing special devices and complex techniques.[1] The most commonly used CR systems are osmotic pump systems, coating techniques, and reservoir devices.[2,3] The high cost of the equipment used, in addition to the complexity of the methods employed, present a tangible problem for continuous, large-scale manufacturing of CR systems. Arguably, monolithic systems (where the drug is dissolved/dispersed in a polymeric matrix) constitute a more convenient alternative

compared to relatively complicated CR device preparation methods.[4] They offer the advantage of utilizing conventional dosage form manufacturing processes using equipment commonly available in any pharmaceutical manufacturing facility.[5] Synthetic and natural polymers are often used for the preparation of such dosage forms. Natural polymers are preferred since they are abundant, biocompatible, biodegradable and cost-effective.[6] Commonly used natural polymers in CR systems include derivatives or salts of cellulose, chitosan, alginate, xanthan gum (XG) and galactomannan.[7–9]

XG is recognized as one of the most efficient natural occurring polymers for use in retarding the release of active pharmaceutical ingredients (APIs) owing to its high water uptake ability and stability against enzymatic degradation in the gastrointestinal tract.[10,11] In addition, XG is biocompatible and is fully degraded by the bacteria of the colon.[12] It has been employed to control the release of various APIs.[13–15] XG is a branched hetero-polysaccharide which is produced by the microorganism species *Xanthomonas*.[5] It is composed of a cellulosic backbone and side-chains consisting of two D-mannose and D-glucuronic acid moieties, in addition to a pyruvic acid group on about half of the terminal D-mannose monomers.[16] Native XG displays an ordered single or double helical conformation which is stabilized by intramolecular hydrogen bonds.[17] In solution, repulsion occurs between XG chains due to the ionization of acidic glucuronic and pyruvate functional groups; thus, XG adopts a flexible coil conformation.[18] Increasing the concentration of ionic species in solutions of XG causes the renaturation of XG to a rigid double-stranded helix conformation.[19] As a result, the water uptake ability of XG is reduced and a greater fraction of the incorporated API is released from the matrix.[20] The high dependence of XG gelling and release behavior on ionic strength hampers its widespread utilization in drug delivery.[18] Attempts to overcome this drawback were the impetus for combining XG with a second polymer i.e., to minimize the effect of the surrounding environment and enhance the drug retardation properties of XG. A wide variety

of polymers have been investigated for such purposes e.g., galactomannan, guar gum, HPMC, starch, PVA, carrageenan, Carbopol and gellan.[11,21–23] Such polymers are either anionic or non-ionic and interact with XG via weak van der Waals intermolecular forces attaining a synergetic CR effect with XG;[24] hence, enhancing the overall retardation of APIs. Therefore, the drawbacks found in the use of each individual polymer are less pronounced, but not eliminated. Owing to the anionic nature of XG, the combination of chitosan (CS) and XG has been widely investigated to control the release of APIs and biomolecules. The unique positive net charge of CS in addition to its other favourable properties, such as biocompatibility and muco-adhesivity, makes it one of the most investigated co-polymers with XG.[25] XG-CS binary mixtures form an insoluble gel layer when exposed to aqueous media.[26] This is due to polyelectrolyte complexation between oppositely charged functional groups of CS and XG.[27] The aforementioned combination has been found to provide a CR effect with a wide range of drugs.[28–31] In the literature, the focus of the majority of the research conducted has been on CR drug delivery utilizing high molecular weight chitosan (HCS) with XG. Most of the results reported demonstrate that in order to exert the highest drug retardation effect, CS is best used with XG at a weight fraction of 50%.[9,20,32] Although the forgoing matrix was capable of hindering the release of incorporated drugs, the drug release displayed a pH-dependency behaviour and was affected by the ionic strength of the dissolution media. Few reports in the literature have considered the pH dependency of CS matrices as an advatange to develop targeted drug delivery systems.[33,34] Others have attempted to overcome this shortcoming by altering the chemical structure of CS. Chemical modification of CS has been used to enhance a specific physicochemical property such as solubility, stability or biological effects e.g., mucoadhesion, cell penetration and antimicrobial effects.[35–37] Since the molecular weight (MW) of CS is the major contributor toward its solubility and interaction with other molecules, low molecular weight chitosan (LCS) has been prepared and studied in the literature in order

to address the effect of MW on the drug release behaviour from CS-XG matrices. The MW of CS has a profound effect on the water uptake capacity of CS-XG matrices.[38] HCS exhibits low water absorption capacity from the dissolution media when compared to LCS. The increase in water absorption causes the formation of more polyelectrolyte complex (PEC) layers which results in potentially more drug retardation. In addition, lower release rates of diclofenac sodium were obtained when incorporated in XG tablets comprising LCS (13 and 30 kDa).[39] Another study confirms the previous finding whereby terbutaline sulfate showed slower release from XG-LCS compared to XG-HCS.[30] Although LCS in the aforementioned studies showed a better CR effect than HCS when combined with XG, a full optimisation of the formulation and a detailed study of its effect on XG sensitivity to pH and ionic strength were not addressed. Metoprolol succinate (MS) was selected as the model drug in this study due to its high aqueous solubility and short biological half-life. MS is a cardio-selective β-blocker used to manage angina, acute myocardial infarction, hypertension and to prevent heart attacks.[40] It is a class I drug, according to the Biopharmaceutics Classification System (BCS), that shows rapid absorption from the GIT following oral administration.[41] Due to its quite short biological half-life (3-7 h) and rapid absorption, metoprolol serves as an ideal candidate for oral CR delivery. Since metoprolol free base is considerably unstable, metoprolol tartrate and succinate are the most common salts used for tablet preparations. MS (Figure 1) is available as a CR product marketed by AstraZeneca (Betaloc® ZOK). Therefore, it was considered as the reference formulation to test the suitability of the drug release matrix.

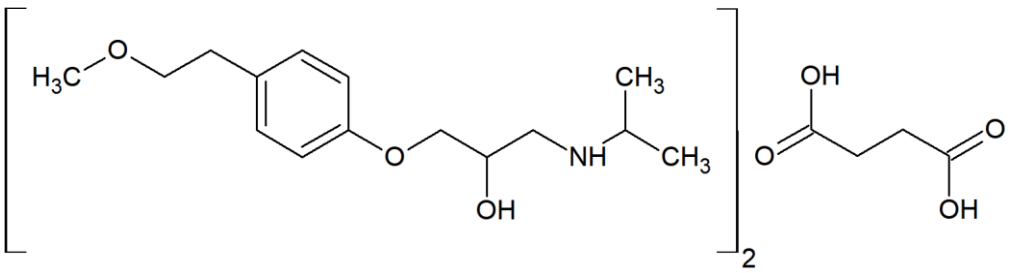

Figure 1 Schematic of the chemical structure of MS.

The objective of the current work was to use scientific evidence to design, formulate and optimize a CR solid matrix system based on polymers, LCS and XG, from biological sources. The foregoing was achieved by: (i) utilizing computational tools/molecular dynamics (MDs) simulations to achieve a broad understanding of the molecular interaction(s) between the studied biopolymers in a way that helps to predict and design the experiments, (ii) evaluate the factors involved in the CR performance of the prepared matrices, and predict the set of parameters that will result in the optimum CR effect using response surface method (RSM), (iii) address the superiority of LCS over HCS in controlling the release of APIs from XG-CS based matrices and in overcoming the limitations of XG as a CR agent, and (iv) employing Raman mapping to evaluate the performance of the prepared matrix and obtain an explanation of the tablet swelling process and drug release mechanism from the developed delivery system.

Experimental section

Materials

LCS with average molecular weight of 13 KDa having an average particle size of ~100 µm, viscosity of 11 mPas (1% w/v in water), and degree of deacetylation > 95 % was purchased from G.T.C. Union Group Ltd, China (batch Nº. GC20140503). HCS with an average molecular weight of 150 KDa, average particle size of ~100 µm, viscosity of 150 mPas (1% w/v in water), and degree of deacetylation > 90 % was purchased from the same source (batch Nº. GC20140510). XG having a viscosity range of 1400-1600 mPa, (1% w/v in water), and average particle size of < 180 µm was purchased from Jungbunzlauer GmbH, Ladenburg, Germany (batch Nº. 2504519). USP grade metoprolol succinate (MS) was obtained from Ipca Laboratories Ltd., Mumbai, India (batch Nº. A0337986). Betaloc® ZOK (AstraZeneca AB, Sodertalje, Sweden) was used as a reference product for MS. All other materials and reagents used were of analytical grade and accessed from the Jordanian Pharmaceutical Manufacturing Co., (JPM), Naor, Jordan.

Computational methods (molecular dynamics simulations, MDs)

AMBER11 software was used to run the MDs by employing the GLYCAM06 force field.[42,43] Initial structures and geometries for XG, LCS and HCS were obtained using the carbohydrate builder database tool provided by the official GLYCAM website.[44] Four monomers were used to build the XG molecule whereas LCS molecules, at different XG: LCS ratios, were built as dimers. In the case of HCS, the molecule was built using nine monomers of glucosamine. Atomic charges were obtained from the force field and the protonation state of both polymers was chosen to mimic the in-vitro release experimental conditions (pH 6.8). Each system was then solvated in a TIP3P periodic box water model whereby counter-ions (sodium and chloride) were added to preserve the neutrality of the systems investigated. Periodic boundary conditions were applied. The non-bonded cut-off was set at 12.0 Å and electrostatic interactions were treated using the Particle Mesh Ewald (PME) method.[45] Energy minimization was carried out for each system, followed by heating to 298 K. A total of 50 ns MD simulations were run using the NPT ensemble to a Berendsen thermostat at 298 K and a barostat at 1 atm.

VMD 1.8.6 software was utilized to visualize the resulting MDs trajectories.[46] MDs analysis were performed using the PTRAJ module of the AMBER 11 tools MDs package.[43] Calculations of binding free energy (ΔG) for each complex were conducted using the molecular mechanics/Poisson–Boltzmann surface area (MM-PBSA) method. Equation 1 was used to calculate the binding free energy:[47]

Equation 1.

$$\Delta G = \Delta E + \Delta G_{solv} - T\Delta S$$

where ΔG_{solv} is the free energy of solvation; ΔE is the gas phase interaction energy and is computed as per equation 2, and TΔS is the conformational entropy of the system.

Equation 2.

$$\Delta E = \Delta E_{elec} + \Delta E_{vdW} + \Delta E_{INT}$$

where ΔE_{elec} is the electrostatic energy, ΔE_{vdW} is the van der Waals interaction energy and ΔE_{INT} is the internal energy.

On the other hand, ΔG_{solv} is composed of the sum of polar (ΔG_{PB}) and non-polar (ΔG_{NP}) interactions and is obtained via equation 3.

Equation 3.

$$\Delta G_{solv} = \Delta G_{PB} + \Delta G_{NP}$$

Preparation and characterization of compacts

MS, XG and LCS powders were, separately, passed through a sieve with a mesh size of 250 μm and collected on a 90 μm mesh. Raw polymers as well as mixtures of XG and LCS (at LCS mass percentages of 15, 25, 35 and 50%) were weighed using an electronic balance. Polymer mixtures were used with or without 95 mg of the drug MS. Polymers or polymers with drug were physically mixed and then directly compressed using a single punch tablet press (Manesty, Merseyside, UK). Samples were filled in a 12-mm circular die with flat-faced punches. Compression was carried out at different forces (in the range of 25-45 units as per the scale provided by the tablet press) in order to obtain tablets with tensile strengths of 0.7, 2.4 and 3.7 N/m^2 (± 0.1). Tablet thickness for the formulation constituted of 15 % LCS was 3.7±0.05 mm. The crushing strength of the prepared tablets, which was used for the calculation of tensile strength, was measured using a hardness tester (Pharma Test PTF E. Hainburg, Germany).

Response surface method (RSM)

The simultaneous effect of the percentage of LCS (A) and polymer-to-drug (P: D) ratio (B), as well as tensile strength (C) on the efficiency of LCS-XG matrices as CR carriers for MS were examined by assigning them as independent variables. While the cumulative drug release from tablets at time intervals of 1 (Y1), 4 (Y2), 8 (Y3) and 20 h (Y4) were assigned as the responses (dependent variables). For each variable, three levels were used; lower, middle and upper. The

effect of independent variables upon the responses was described using different polynomial equations for the various measured responses. Design-Expert® software version 10.0.1.0 (Stat-Ease, Inc., Minneapolis, USA) was employed. A total of 27 runs of in-vitro release trials were conducted to collect enough data to build mathematical models and thus generate the necessary contour plots. The goodness-of-fit of the suggested models was established using the coefficient of determination (R-squared, R^2). ANOVA analysis were conducted for the suggested models. A model was considered significant when p-values were less than 0.05.

In-vitro release studies of MS from XG-LCS tablets

In-vitro release studies were conducted using USP apparatus II (Labindia DS8000, Labindia Analytical Instruments Pvt. Ltd., New Delhi, India) in 500 ml phosphate buffer pH 6.8 at 37±0.5 °C and 50 rpm rotation speed; the foregoing parameters comply with USP32-NF27 specifications. Samples (10 ml) were withdrawn at time intervals of 1, 2, 4, 6, 8, 12, 16 and 20 h and replaced with an equivalent volume of the dissolution medium. Sample aliquots were passed through 0.7 µm membrane filters and analysed by UV spectrophotometry (LABINDIA UV/VIS Spectrophotometer UV 3000+, Maharashtra, India) at 274 nm and 2 nm spectral bandwidth. 1 cm quartz cells were used to measure the absorbance of the samples and results were recorded using UVWin 5 software. A stock solution of 1 mg/mL of MS was prepared by accurately weighing 100 mg MS and dissolving it in 100 mL deionized water. Standard solutions were prepared from the stock solution to generate the calibration curve. The UV method of analysis of MS was validated in compliance with the International Conference on Harmonization (ICH) 2QB guidelines for validation of analytical procedures.[48] The linearity (R^2= 0.9999), linear range (40-200 µg/mL), limit of detection (7.8 µg/mL) and limit of quantitation (23.7 µg/mL) for the analysis of the drug were established from the data obtained.

Water uptake (swelling) and matrix erosion measurements of tablets

Tablets were placed in a USP dissolution apparatus II (Labindia DS8000, Labindia Analytical Instruments Pvt. Ltd., New Delhi, India) using the same experimental conditions described in the in-vitro release section. At pre-determined time intervals tablets were detached, carefully blotted on adsorbent tissue to remove excess water and weighed using an electronic balance with a resolution of 0.1 mg (AG245, Mettler Toledo, Ohio, United States). The swollen tablets were left to dry at ambient temperature for 24 h, incubated in a vacuum oven at 25 °C for 12 h before determining the dry weight. Tablets were incubated again in the vacuum oven for an extra 12 h in order to ensure that the weight of the dried tablets was consistent. When needed, the drying cycles were repeated until a constant weight was achieved. The cumulative percentage swelling and remaining mass of the tablets at each time point were determined using equations 4 and 5, respectively.

Equation 4.

$$\text{Swelling (\%)} = \left(\frac{X_{st} - X_0}{X_0}\right) \times 100$$

Equation 5.

$$\text{Remaining mass (\%)} = \left(\frac{X_{dt}}{X_0}\right) \times 100$$

where X_0 is the initial weight of the tablet, whilst X_{st} and X_{dt} represent the weight of the swollen and the dried tablets at time t, respectively.

Evaluating the drug distribution during dissolution using Raman mapping

Raman mapping was used to monitor drug distribution between the two regions (dry core and hydrated gel layer) of the tablets. Swollen tablets were withdrawn from the dissolution vessels at time intervals of 1, 2, 4, 8 and 12 h, carefully blotted on absorbent paper to remove excess water and cut in halves. A Horiba LabRam I spectrometer (Horiba Jobin Yvon Ltd., UK) equipped with an automated XYZ stage (Märzhäuser) and Olympus BX40 microscope was

used in this study. The instrument was calibrated using a silicon band at 520.7 cm^{-1}. Raman spectra were acquired by employing a near-IR laser (785 nm) providing an excitation power of 100 mW, 10× Olympus objective, 1200 lines/mm grating and a Synapse Peltier-cooled CCD detector. Raman maps were generated by collecting the spectra for an area of 720 × 720 μm from each region of the tablets. The grid spacing between each point was 24 μm for both the x-axis and the y-axis, and a total of 900 spectra per map were collected. SWIFT mode was utilized to allow rapid mapping and avoid drug migration between the different tablet layers during measurements. The acquisition time was set to 0.5 seconds per spectrum and the LabSpec 6 (Horiba Jobin Yvon Ltd., UK) software package was used to collect the spectra and maps.

In-vitro evaluation of the effect of pH, ionic strength and the presence of ethanol in dissolution media on the rate of drug release and dose dumping

The impact of ionic strength (μ) on the release rate of MS from the matrix was assessed by adding NaCl to phosphate buffer at concentrations of 0.1, 0.2 and 0.4 M. The effect of pH was evaluated by testing the release of MS from prepared compacts in three different media (pH 1.2, 4.5 and 6.8). In accordance with FDA guidelines,[49] dose dumping studies were carried out in the presence of ethanol. Dissolution tests were carried out using USP II apparatus at 37±0.5 °C and 50 rpm rotation speed. Vessels were filled with 500 ml HCl 0.1N containing ethanol at concentrations of 5, 20 and 40% (v/v). Samples (10 ml) were collected for 2 h and the release of MS from the LCS/XG preparation was compared to the reference product.

Statistical analysis

Calculations were carried out using Excel 2016 (Microsoft, USA). Data represents the mean ± standard deviation. The 2-D schematic structures of the studied compounds were built using ACD/ChemSketch 2017.2.1 (Advanced Chemistry Development, Inc., Toronto, ON, Canada) software. Data plots were generated using Excel 2016 software (Microsoft, USA).

Results and discussion

Molecular dynamic simulations (MDs)

MDs were utilized in this work in order to explain the mechanism of interaction between LCS and XG and to find/predict the XG: LCS ratio that would result in the most favourable interaction between the two biopolymers. In previous MDs work, we reported that electrostatic interactions are responsible for complex formation and stabilization between LCS and XG at a single interaction ratio of 1:1.[50] In addition, we found that protonation of amine groups in LCS is the most important factor affecting the interaction between the two polymers. In the current study, we have extended the previous MDs work and investigated the interaction between LCS and XG at different ratios and at a fixed protonation state in accordance with the pH of the dissolution medium used in the experimental studies. Ratios of LCS/XG were converted from (w/w) to molar ratios to mimic experimental conditions.

Root mean square deviation (RMSD) data indicates how far molecules have migrated from their initial structures during the MDs (Figure 2a). It was found that complexes with LCS values ≥ 25% exhibited a pronounced deviation from their initial structures with high fluctuations, from about 8 to 22 Å, during the MDs. Complexes with lower percentages of LCS, 15%, displayed lower movement (< 10 Å) with minor fluctuations. The observed deviations, which indicate instability of the resultant complexes, was in the order 50 > 35 > 25 > 15% of LCS. Importantly, the fluctuation in the mean distances decreased after ~ 10 ns for LCS/XG complex constituted of 15% LCS and ~ 30-40 ns for complexes composed of 25-50% of LCS indicating that the systems need 30-40 ns to stabilize and equilibrate during the MDs. Thus, the average structures and energy calculations were computed for the last 10 ns of the resultant trajectories.

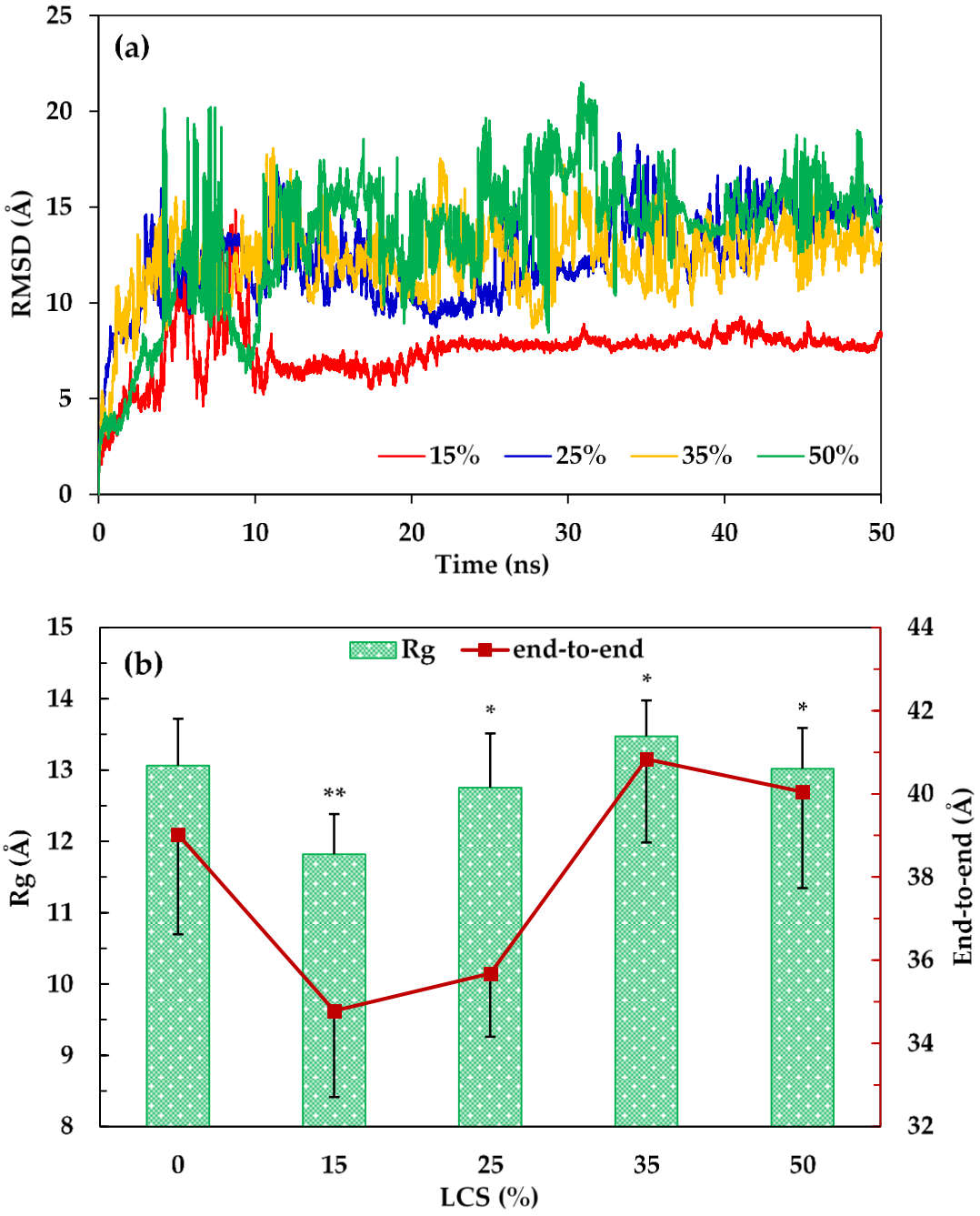

Figure 2 (a) RMSD values for LCS-XG mixtures; values on the lower right corner represent the % LCS (w/w). (b) Calculated average Rg and end-to-end distance values for XG chains during the 50-ns simulation of LCS-XG mixtures at different % of LCS. Error bars represent SD values, * *denotes insignificant differences in the average Rg values of LCS-XG complexes from the average Rg value of XG alone (0% LCS, p>0.05), whereas ** denotes a significant difference (p<0.05).*

The average structure of each polymer mixture showed that LCS molecules are embedded between the backbone and the peripheral chains of XG (Figure 3). Increasing the number of LCS molecules resulted in a less favoured interaction between the two polymers in which less contact with XG was found in polymer mixtures with LCS content of > 25%.

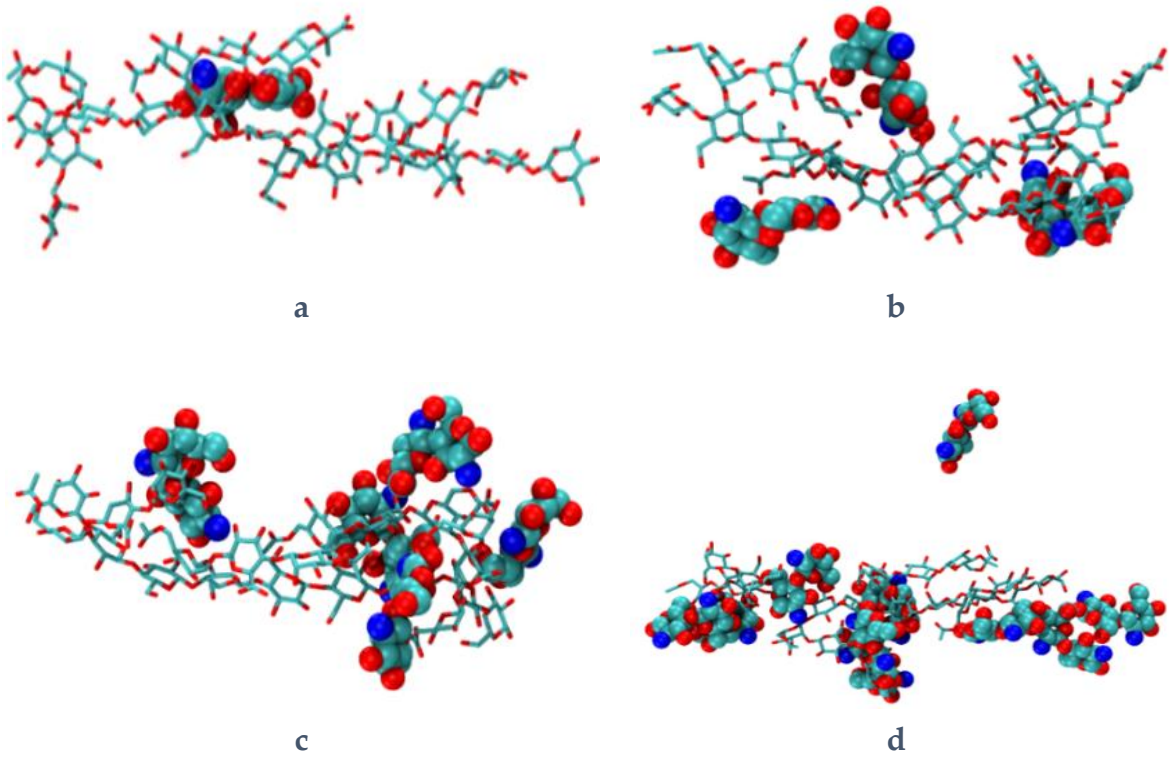

Figure 3 Average structures of LCS-XG mixtures obtained using MDs at LCS values of: (a) 15, (b) 25, (c) 35, and (d) 50%. XG is represented in line model mode whereas LCS is represented in the VDW model mode. Hydrogen atoms were excluded for clarity, oxygen atoms are displayed in red, carbon in cyan, and nitrogen in blue.

Molecular mechanics/Poisson–Boltzmann surface areas (MM-PBSA) was used to compute the binding free energies of the studied complexes (Table 1). Results revealed that electrostatic forces (polar interactions) between the two polymers are the major contributor towards the formation and stability of LCS-XG complexes, which is in accord with our previous work.[50] The existence of oppositely charged groups, NH_3^+ in LCS and COO^- in XG, in the structure of the polymers gives rise to the electrostatic forces. Increasing the content of LCS resulted in a higher positive charge density within the mixture, owing to the cationic amine groups. As a result, repulsion between LCS molecules occurs causing a substantial increase in the movement and fluctuation of atoms when the LCS content is > 25%, as was addressed by RMSD results. Hence, the contact and interaction of LCS molecules with XG decrease and less stable complexes are formed. To a much lower extent, Van der Waals forces (ΔE_{vdW}) also play a role in the formation of LCS/XG complexes having values less than one tenth of ΔE_{elec} values. The

positive values of the solvation free energy (ΔG_{solv}) demonstrate the formation of insoluble complexes between LCS and XG at all ratios. The total free energy of binding (ΔG) was computed for the studied complexes. ΔG values are negative for all complexes indicating favourable interactions between LCS and XG at all mixing ratios. However, it is noticeable that increasing the fraction of LCS results in less favourable interactions, which correlates well with both the RMSD results and the average structure snapshots. The most stable complex between LCS and XG is formed at LCS contents of 15%. It is noticeable that the total interaction energy (ΔE) between XG and LCS increases with the % LCS, indicating more deviation of the molecules from their initial structures. However, ΔE values are compensated by the high negative entropy (TΔS) values which suggests a reduced conformational flexibility of the molecules upon complexation. Thus, XG and 15% LCS formed the most favourable complex. Increasing LCS content to 25% resulted in ~ 8 kcal/mol decrease in ΔG. No significant decrease in ΔG values were found in LCS-XG mixtures containing > 25% LCS comparing to 25% LCS.

Table 1 MM-PBSA results for the LCS-XG mixtures at different % (w/w) of LCS.

LCS (% w/w)	ΔE_{elec}[a]	ΔE_{vdW}[a]	ΔG_{solv}[a]	ΔE[a]	$T\Delta S$[a]	ΔG[a]
15%	-256.41 ± 45.8	-18.11 ± 05.5	249.49 ± 36.6	-25.04 ± 11.8	3.35[c]	-28.39
25%	-484.72 ± 75.9	-43.70 ± 10.8	484.68 ± 70.9	-43.76 ± 0.13	-23.09	-20.65
35%	-620.20 ± 46.5	-47.14 ± 06.9	616.41 ± 43.9	-50.63 ± 0.14	-30.98	-19.65
50%	-1747.9 ± 63.6	-90.02 ± 09.1	1720.1 ± 59.2	-117.8 ± 16.6	-97.45	-20.35
HCS[b]	-604.56 ± 57.9	-55.63 ± 08.8	655.33 ± 62.4	-04.99 ± 04.7	-31.50	26.61[c]

[a] Values shown are in kcal/mol. [b] Energy values represent the MMPBSA results for a single chain HCS molecule with XG. [c] Note that these values are positive.

In order to elucidate the conformational flexibility of XG during MDs, the radius of gyration (Rg) and end-to-end distances of XG chain were calculated for all complexes (Figure 2b). Rg is a property that describes the conformational flexibility of polymers; it gives an indication of whether the polymer chains are extended or folded. Average values of Rg and end-to-end distance for XG exhibited a decrease in both 15 and 25% LCS complexes compared to the

values obtained from XG alone (0% LCS), being more pronounced in XG-LCS 15%. This suggests a flexible conformation of XG whereby the chains are folding to interact with LCS. This is in accord with results obtained from the average structure, indicates that the system is reaching equilibrium[51] and that the interaction between XG and LCS is favoured, as shown by the free energy values. A restriction in the flexibility of XG can be noticed when increasing the ratio of LCS to 35% with the backbone being more extended causing a reduction in the contact with LCS which is obvious from both the average structure and MMPBSA results. When the LCS ratio reached 50%, a slight reduction in the Rg and end-to-end distance values of XG was noted compared to the 35% LCS complex suggesting either no change in the conformation of XG when LCS is incorporated at percentages ≥ 35%, or that the maximum extended structure of XG was obtained when combining it with LCS at 35%. This is in accord with the MMPBSA results which suggest that the least favourable complex is formed when the LCS ratio is 35%.

To justify the chosen molecular weight of CS and assess the benefit of using LCS compared to HCS, an MD simulation was carried out between XG and HCS using a single long-chained CS molecule (9 monomers). The average structure, Figure 4a, exhibited good contact between the HCS and XG molecules. However, RMSD calculations (Figure 4b) showed a higher deviation from the starting structure compared to the MD simulation data for XG with a single LCS molecule (dimer). In addition, a high fluctuation can be noticed for the first 30 ns of the HCS trajectory whereas the LCS took around 10 ns to reach equilibrium and the most favourable conformation. End-to-end distance of the XG backbone was measured from both LCS and HCS trajectories to address the effect of CS molecular weight on the flexibility of XG during MDs. It can be noticed from the data presented in Figure 4c that the XG chain is more flexible and favours a more folded structure when allowed to interact with LCS, reaching distances as low as 25 Å, whereas when it was interacted with HCS a more rigid and expanded structure was obtained with an average end-to-end distance of ~ 43 (Å).

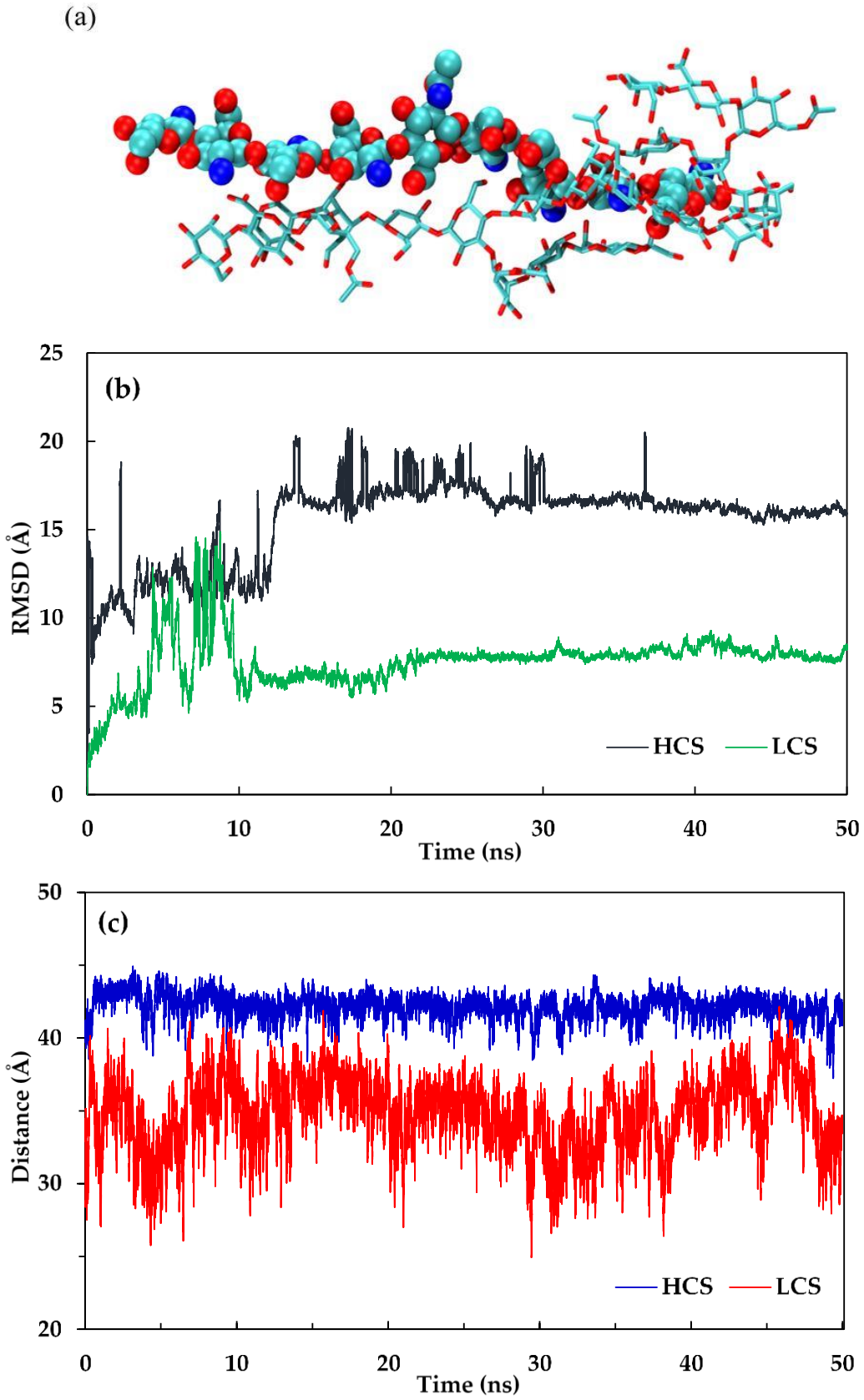

Figure 4 (a) Average structures of HCS-XG obtained from 50 ns MDs. The XG molecule is presented in line model mode, whereas HCS is in the VDW model mode; (b) RMSD values obtained during the simulation time for complexes comprising XG with a single LCS dimer and HCS molecules; (c) end-to-end distance values calculated for the XG backbone during the 50-ns MDs with LCS and HCS.

A plausible explanation for the results obtained is that LCS retains the backbone structure of HCS but displays a less crystalline structure.[52] In addition, intra-molecular hydrogen bonds and Van der Waals forces are reduced as a result of decreasing chain length.[53] Consequently, the free mobility of LCS molecules is increased, they become soluble in water/neutral solutions, and interact more readily with other molecules.[5] Therefore, LCS was used with XG to optimize and evaluate a hydrophilic solid matrix to control the release of the model drug MS.

Response surface method (RSM)

Response surface method (RSM) is a design of experiment tool that is used to gauge the significance of each selected factor on the responses and to predict the correlation and interaction between experimental variables so that the response can be optimized accordingly.[54] In addition, it offers the advantage of weighing the effect of several variables on more than one response at the same time. RSM was utilized to test our MDs findings of the optimum mass fraction of LCS and to optimize the final formulation depending on the effect of the P:D ratio and LCS% at different tensile strength values on the retardation efficiency of the formed compacts. All input variables were subjected to multiple model fitting and linear regression followed by ANOVA to find the model that shows the best correlation between predicted and actual values. Probability p-values < 0.05 indicate the significance of the model whereas the f-value relates the outcomes to the noise in which values > 3.5 imply an adequate significance of the model over the noise (as specified by Design Expert®). Adequate precision (Adeq pre) measures the signal to noise ratio; a value greater than 4 is desirable. In general, the higher the R-squared (R^2) value the better the model fits the data. A difference between predicted R-squared (Pred R^2) and adjusted R-squared (Adj R^2) of less than 0.2 indicates the validity of the selected model. Generated polynomial models and equations imply the high dependence of drug release from the matrix on both the percentage of LCS (A) and the P:D (B) values. The analysis showed that the best goodness-of-fit result was obtained for the quadratic

polynomial model. The summary model data for each response is presented in Table 2. Calculated p, f and adequate precision values denote the significance and the validity of the quadratic polynomial model in describing the correlation between independent variables and responses. Generated equations can predict from 91% (Y4) up to 99.5 % (Y1 and Y2) of drug release data points as implied by R^2 values.

Table 2 Summary data for each model and ANOVA results of studied variables and responses.

Response	p-value	f-value	R^2	Pred R^2	Adj R^2	Adeq pre	Equation*
Y1 (1 h)	0.0001	367.67	0.9949	0.9876	0.9922	45.61	$Y1= 18.21+40.14A-4.71B-1.8C-8.036\times10^{-3}AB+0.34AC-0.45BC+36.51A^2+2.48B^2+1.17C^2$
Y2 (4 h)	0.0001	353.04	0.9947	0.9854	0.9919	52.69	$Y2= 55.43+30.19A-4.22B-2.89C+2.55AB+2.34AC-0.37BC+11.59A^2+1.46B^2+1.90C^2$
Y3 (8 h)	0.0482	107.71	0.9828	0.9560	0.9736	31.71	$Y3= 75.64+19.77A-5.14B-1.85C+3.76AB+1.07AC-0.028BC+3.36A^2+0.048B^2+1.31C^2$
Y4 (20 h)	0.0009	19.250	0.9107	0.7682	0.8634	16.90	$Y4= 98.89+4.34A-1.04B-2.05C+1.49AB+2.92AC-0.16BC-3.80A^2+0.24B^2+0.79C^2$

** Dependent variables are: (A) LCS%, (B) P:D, and (C) tensile strength*

Contour plots illustrating the design space (blue area) and showing the effect of LCS% (A) and polymer to drug P:D ratio (B) on the release of the drug from XG-LCS tablets at different tensile strengths (C) are presented in Figure 5. Acceptance criteria data for the release of MS from controlled-release tablets, as specified by USP32-NF27, are presented in Table 3. The initial release of MS after 1 h shows that tablets containing up to 50% LCS at any P:D ratio meet the USP criteria. With the lapse of time, in relation to responses (Y2 and Y3) which represent time intervals (4 and 8 h, respectively), the design space that fulfils USP requirements was narrowed (blue area). At low tensile strength (0.7 N/m^2), the design space was limited to the use of no more than 15% LCS at a P:D ratio of 4:1 after 8 h, whereas if a P:D ratio of 3:1 was adopted, pure XG should be used to control the release of MS. Increasing the tensile strength to 3.7 N/m^2 resulted in more flexibility in design space allowing the incorporation of around 25% LCS and a total P:D ratio of 2.2:1. Tablets at all P:D ratios and % LCS showed almost full release (≥ 88%) of the incorporated drug dosage after 20 h of dissolution.

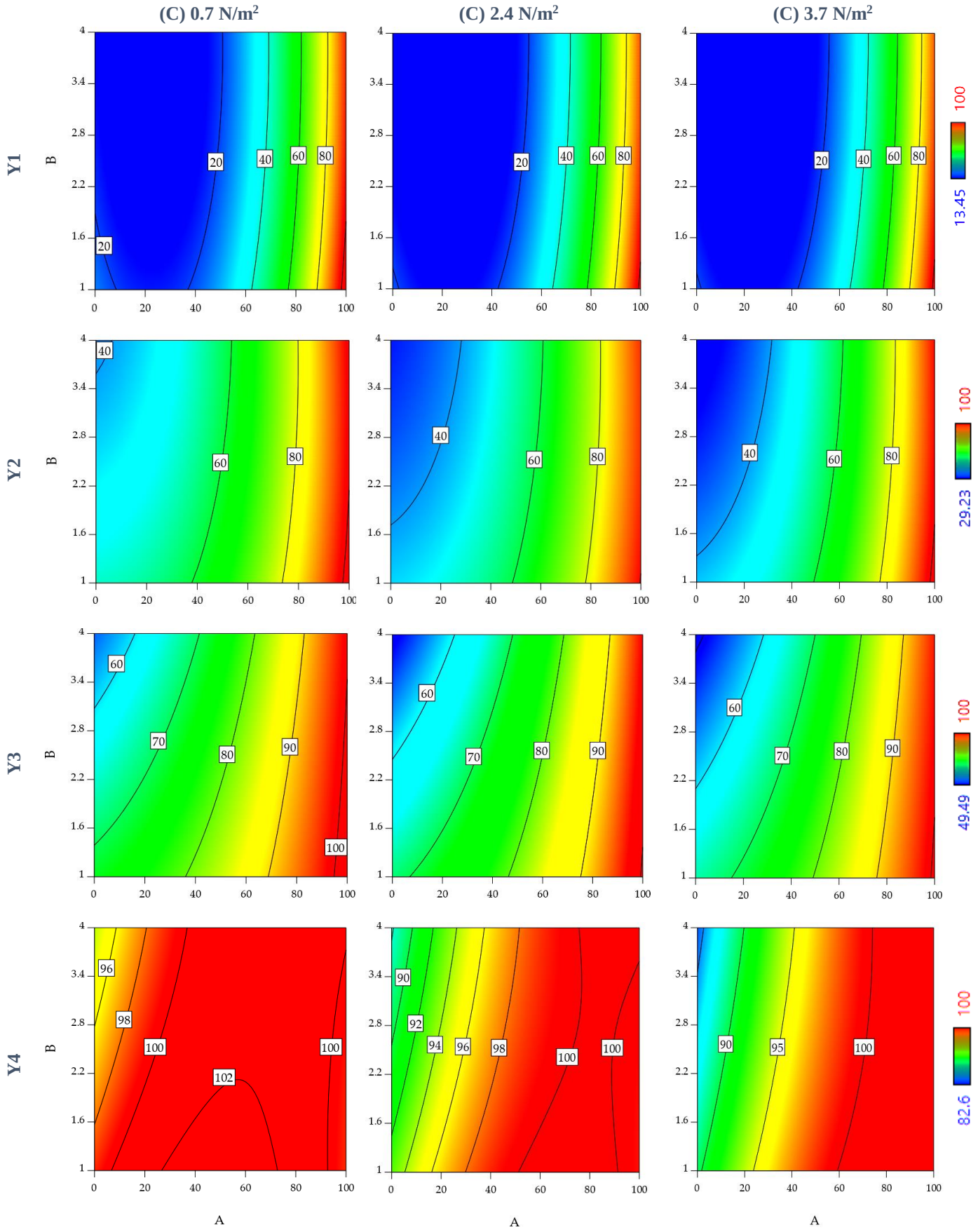

Figure 5 Contour plots of drug release from LCS-XG based tablets as a function of (A) % LCS, (B) P:D ratio and (C) tensile strength of prepared tablets at: (Y1) 1 h, (Y2) 4 h, (Y3) 8 h, and (Y4) 20 h.

Table 3 USP acceptance criteria for MS controlled release tablets.

Time (h)	Amount dissolved
1	NMT* 25%
4	20% - 40%
8	40% - 60%
20	NLT** 80%

** NMT: not more than, and ** NLT: not less than*

The results obtained from RSM are in accordance with the results of Mundada et al. who found that the P:D play a major role in controlling the release of MS using various cellulosic and acrylic polymers derivatives.[55] In addition, Gohel et al. reported a high dependency of MS release rate from wet granulated tablets on the ratio of XG and HPMC in the tablet.[56] This can be explained by the longer path MS needs to travel when the ratio of the polymer(s), XG and LCS in our case, is increased in the tablet.[57]

The overall design space (yellow area, Figure 6) for the optimum release of MS from XG-LCS based tablets at a tensile strength of 2.4 N/m^2 (which was adopted in this study) suggests that at a P:D ratio of 4:1 the ability to control the release of MS can be exerted using LCS at percentages up to around 20%. When using the lowest possible P:D ratio in the design space (~ 2.6:1), the model output endorses the use of XG alone to maintain the retardation efficiency of the matrix. Hence, in order to examine the advantage of incorporating LCS in the preparation, further in-vitro evaluation (swelling and dissolution studies) were carried out.

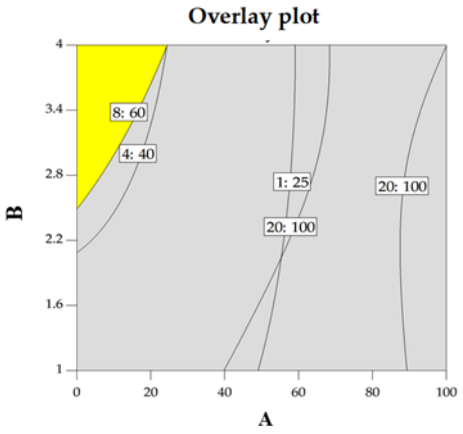

Figure 6 Design space (yellow area) representing the optimum combination of variables for the CR delivery of MS from LCS-XG tablets. (A) LCS (%) and (B) P:D ratio. (C= 2.4 N/m^2).

In-vitro release dissolution and tablets swelling studies

The in-vitro release profiles for MS from LCS-XG tablets at different mass fractions of LCS are presented in Figure 7a. A P:D ratio of 4:1 was adopted from the design space obtained using RSM (Figure 6). MS showed an immediate release pattern when incorporated with LCS as the sole polymer. This behavior was expected since the retardation ability of hydrophilic polymers is directly proportional to their viscosity (molecular weight).[58] Therefore, LCS alone is not suitable for drug retardation and the maximum used weight percentage was limited to 50%. On the other hand, XG was able to retard the release of MS. Tablets prepared from the binary biopolymers mixture were capable of sustaining the release of MS at all incorporated LCS mass ratios. The pattern of drug release was inversely proportional to the % LCS. Almost half of the incorporated drug dose was preserved in tablets containing 15% LCS after 8 h, whereas ~85% of the dose was released after 8 h from tablets constituted of 50% LCS. This is in agreement with the findings of Varshosaz et al who examined the release of MS from tablets comprising XG with guar gum.[59] They found that tablets containing higher ratios of XG displayed higher drug retardation ability.

The drug retardation capability of LCS/XG mixtures can be explained by polyelectrolyte complexation. Once tablets are in contact with the dissolution medium, PECs start to form between XG and LCS on the surface of the tablets. This is due to ionic interactions between the oppositely charged polymers.[26] This was confirmed by the outcomes of MDs which showed that the main contributor for the interaction between XG and LCS is electrostatic forces. Although the formed PECs are physically cross-linked, they were able to render the release of MS from the LCS-XG matrices. Thus, PECs can serve as alternatives to chemically cross-linked hydrogels (using e.g., chemical cross-linkers such as glutaraldehyde) offering the advantage of biocompatibility.

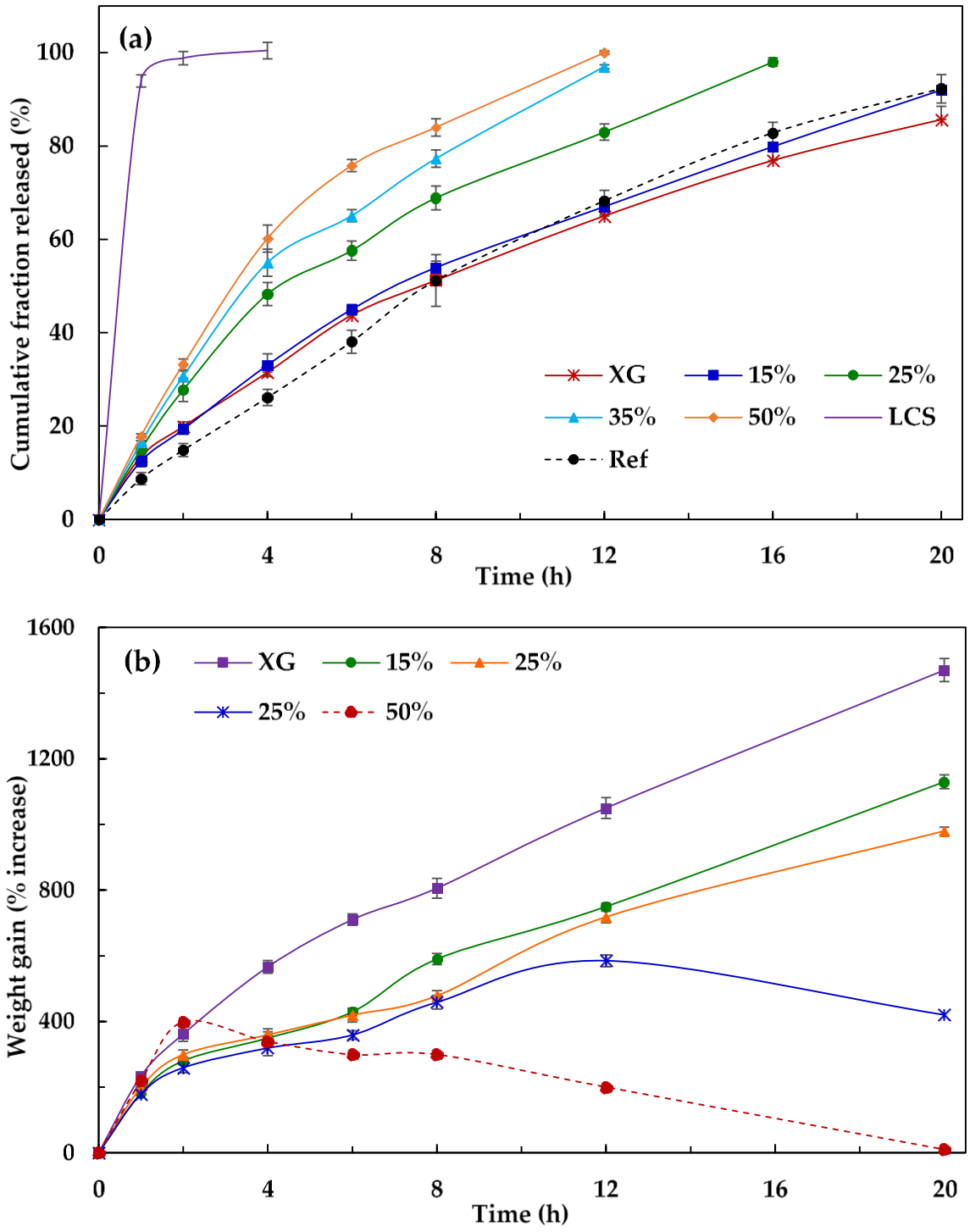

Figure 7 (a) In-vitro release profiles of MS from prepared compacts and the reference product, Betaloc® ZOK in phosphate buffer pH 6.8. *Values represent mean ± SD (n=12);* (b) Degree of swelling of the XG and LCS/XG matrix tablets in phosphate buffer, pH 6.8. *Values represent mean ± SD (n=6).*

The percentage weight gain (swelling) of the hydrated XG-LCS matrices was measured for 20 h (Figure 7b). Pure XG showed rapid and high levels of hydration where the tablet weight kept increasing, reaching almost 1500% of its initial weight after 20 h. This behavior was

predicted considering the high-water uptake capacity and rapid weight gain of tablets comprising XG.[56] In contrast, LCS based tablets fully disintegrated within the first hour of the experiments showing no hydration capability. Thus, measurements for the degree of swelling were not obtainable for LCS. This is in accord with the immediate release behavior of LCS formulations in dissolution studies and with the results of Ritthidej et al., who investigated the capability of using CS as a disintegrant in tablets and found that CS can be used as an effective disintegrant in tablet formulations.[60] In the case of LCS/XG matrices, it is obvious that mixtures containing lower levels of XG (35% and 50% LCS) showed a minor weight gain followed by a marked weight loss, as a result of the disintegration of LCS. On the other hand, mixtures containing 15-25% LCS showed high swelling capacity but to a lower extent than XG. This can be explained by the distribution of LCS molecules between XG chains, as illustrated in Figure 3, which lowers the contact between water molecules and XG; hence, swelling was reduced.

Based on the results obtained from MDs, RSM, swelling and in-vitro release studies, the optimum release of MS, which complies with the USP specifications, was attained using a formulation containing 15% LCS (w/w). Thus, it was compared to the reference preparation (Betaloc® ZOK). Similarity factor, f_2, was calculated for the comparison using equation 6.

Equation 6.

$$f2 = 50\log\left\{\left[1 + \left(\frac{1}{n}\right)\sum_{t=1}^{n}(R_t - T_t)^2\right]^{-0.5} \times 100\right\}$$

where n is the number of time intervals, t is time, R_t and T_t are the accumulative percentages of drug release at time t for reference and test formulations, respectively. According to the guidelines, f_2 values greater than 50 indicates a similar release profile between the two studied formulations,[61] the f_2 value for the 15% LCS formulation was 68 indicating a high similarity in the release of MS from the formulation with the reference product.

Tablet preparations containing 15% of LCS were used for further evaluation and investigation of swelling and drug release characteristics. Dissolution data obtained for MS were fitted to different release models in order to evaluate the kinetics of drug release from the matrix.[62,63] The in-vitro release mechanism of MS from the 15% LCS formulation (Table 4) showed a good fit to zero-order, first-order and Higuchi models ($R^2 > 0.95$). This indicates the complexity of the prepared delivery system where different mechanisms are involved in MS release from the LCS/XG matrix.

Table 4 In-vitro release parameters for MS from 15 % (w/w) LCS matrix tablets.

Formulation	Correlation coefficient (R^2)				Release exponent (n)
	Zero-order	First-order	Higuchi	Koresmeyer-Peppas	
15% LCS	0.952	0.989	0.966	0.992	0.63

In general, the mechanism of drug release from hydrophilic matrices is governed by: (i) wetting of the surface of the tablet, (ii) penetration of the media into the tablet, (iii) hydrogel formation (swelling), (iv) drug diffusion through the formed hydrogel, and (v) polymer relaxation and/or erosion.[58,64] Considering the hydrophilic nature of LCS and XG in addition to the formation of an insoluble hydrogel layer (PEC) on the surface of their corresponding tablets, release is proposed to be governed by the swelling of the matrix to form the PEC layer and the diffusion of the drug through the insoluble layer formed. The Koresmeyer-Peppas exponent (0.63) for the 15% LCS preparation supports the hypothesis that the release of MS occurs via non-Fickian diffusion, which suggests that the diffusion of water molecules into the matrix together with polymer relaxation due to swelling are the factors that control the rate of MS release from the matrix.

The data in Figure 8, shows that the radius of the tablets started to increase from the beginning of the dissolution process reaching the maximum radius after 12 h. This implies that the diffusion of water molecules plays an important role in drug release in the first 12 h of the dissolution process. After 12 h, the tablet was full hydrated and polymer relaxation reached a

maximum. Importantly, at the start of tablet dissolution and prior to complete film formation (0-2 h), around 12% of the tablet was eroded (6%/h), whereas during the stage of diffusion and polymer relaxation (2-12 h), a significant decrease in the rate of matrix erosion was noticed (0.7%/h) and only ~7% of the matrix was eroded. This indicates that the formation of PECs between XG and LCS prevents further polymer erosion and minimize its effect on drug release from the tablet.[65] In the later stages of dissolution, the rate of polymer erosion was slightly increased (~1.8%/h) and the remaining mass of tablets at the end of the dissolution process was ~ 65%.

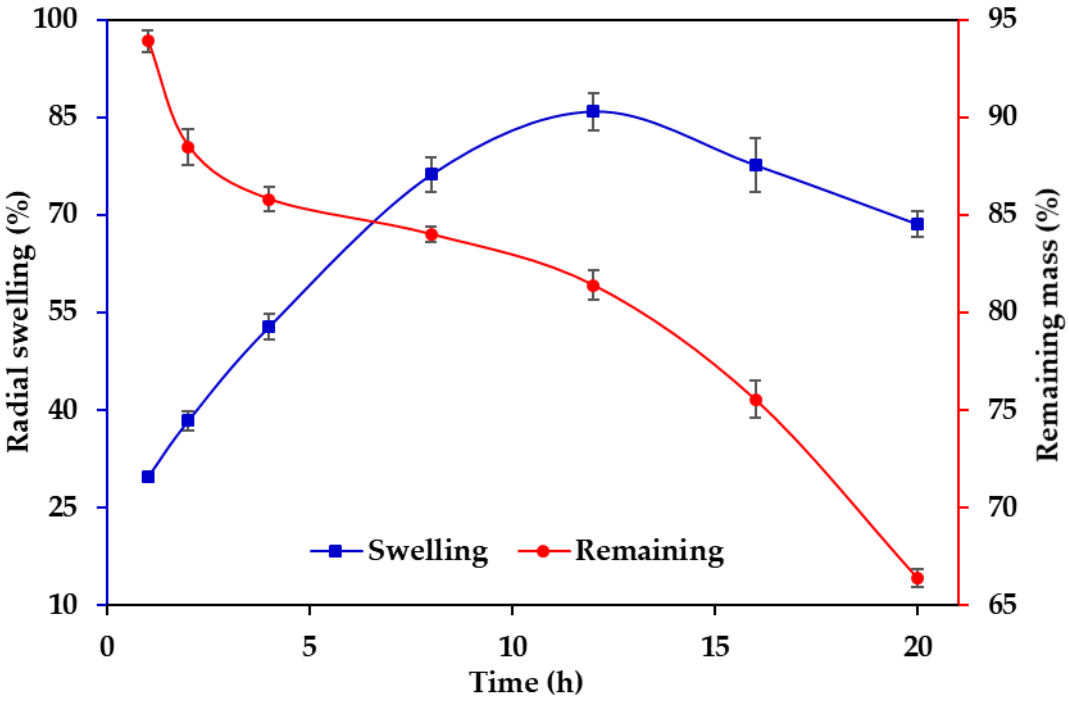

Figure 8 Remaining mass (red) and radial swelling (blue) % increase of the 15% LCS tablets during dissolution in phosphate buffer. *Values represent mean ± SD (n=6).*

To test the suggested MS release mechanisms and assess the significance of diffusion and polymer relaxation processes on the release, the Peppas-Sahlin equation (Equation 7) was used.

Equation 7.

$$Q = k_1 t^m + k_2 t^{2m}$$

where Q is the rate of drug release. The first term on the right-hand side of the equation represent the Fickian diffusion contribution, while the second term represents the polymer

relaxation contribution; k_1 and k_2 are the diffusion and relaxation rate constants, respectively and m is a constant that is related to the CR system. Results are presented in Table 5. Since $k_2 > k_1$, it can be concluded that polymer relaxation (swelling) mechanism is the predominant mechanism for the drug release from the 15% LCS formulation. This is in agreement with the work of Gohel et al. who found that the release of MS from tablets containing XG, as the sole drug release controlling agent, is governed by XG relaxation.[56] On the other hand, when non-ionic natural polymers were used to sustain the release of MS (guar gum and badam gum), drug diffusion was the dominant factor in the control of the rate of release of MS from the tablets.[59,66]

Table 5 Pappas-Sahlin release parameters for MS from 15 % (w/w) LCS matrix tablets.

Formulation	**k_1**	**k_2**	**m**	**R^2**
LCS 15%	-22.88	34.45	0.23	0.9975

Evaluation of drug distribution during dissolution using Raman mapping

Imaging and mapping of APIs using vibrational spectroscopy methods have gained wide interest in the field of pharmaceutical formulation and process analytical technology. Vibrational spectroscopic techniques, infra-red and Raman spectroscopy, allow the continuous monitoring of APIs during processing which helps to evaluate the effect of formulation variables on the final product performance.[67,68] Recently, vibrational spectroscopy techniques have been employed in tablet dissolution studies in order to obtain a better understanding of the process of drug release from pharmaceutical formulations and to monitor drug distribution within it.[69,70] Since the Raman intensity of water is very weak compared to IR,[71] Raman spectroscopy was chosen to monitor MS distribution between the dry core region and the hydrated gel layer during the time of swelling/dissolution. Raman spectra of pure MS, LCS and XG were obtained to determine the characteristic Raman shifts to be used during mapping to distinguish MS from the polymeric mixture (Figure 9). The model drug, MS, showed several characteristic vibrational bands in which it can be distinguished from the polymeric mixture.

The most intense vibrational bands appeared at 818, 964 and 1209 cm^{-1}. Therefore, Raman mapping was performed in the region between 700 and 1400 cm^{-1}.

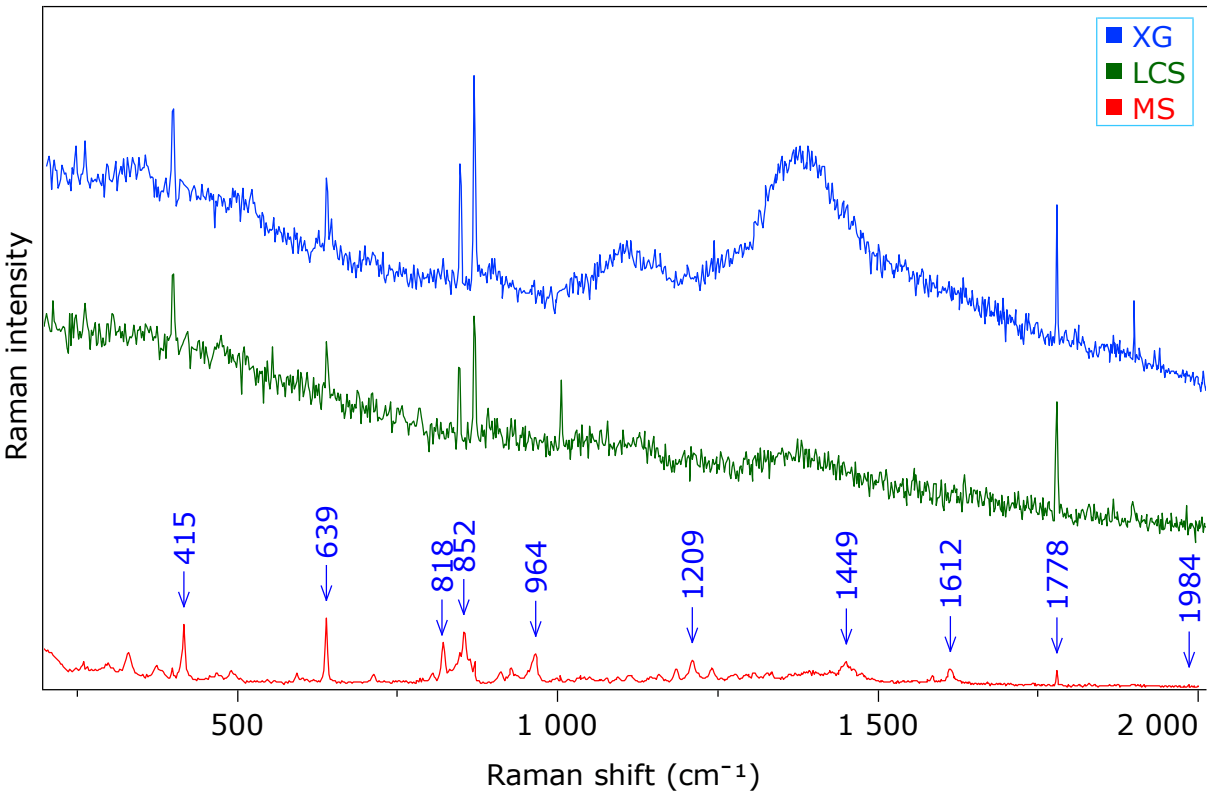

Figure 9 Raman spectra of MS, LCS and XG powders using a 785 nm laser.

Figure 10 shows the morphological changes in the course of dissolution time on the surface of LCS-XG tablets and the drug distribution between the core and the gel layer during tablet dissolution. The highest concentration of the drug within the mapped area is presented in red whereas the lowest is represented in blue. It can be noticed that MS was more localized in the dry core for the first 4 h of the dissolution. A very small fraction of the drug migrated from the dry core to the gel layer at 1 h. Since the tablets were formulated from a physical mixture of the polymers where the drug is uniformly dispersed within the matrix, the fraction of the drug in the gel layer could be the fraction that was already available in the outer part of the tablet when the polymers started to absorb water from the dissolution media. A higher fraction of the drug moves from the core to the hydrogel layer with time reaching an almost equal distribution between the two layers after 8 h of dissolution. By that time, tablets became almost fully

hydrated, and it was difficult to distinguish the core from the hydrated layer. After 12 h, tablets were fully swollen and hydrated with no different regions. Thus, Raman mapping was carried out for 12 h.

Snapshots from the video images of the top surface of the tablets were recorded during dissolution to monitor PEC formation between XG and LCS. It can be noticed that after 1 h of dissolution a film started to form on the top surface of the tablets. The formation of the film was complete after 2 h and its integrity was maintained at 4 h. Film formation on the surface of tablets is verified by data in the literature.[64] It was found that tablets comprising CS and anionic polymers such as XG, sodium alginate and carrageenan can form films on tablet surfaces during dissolution. Phaechamud and Ritthidej reported the formation of a porous film on the surface of tablets comprising CS-XG. They noted that the film was denser after 4 h of dissolution and suggested that it plays a role in drug diffusion and release into the media.[72] Shao et al., found a profound reduction in swelling and erosion ratios of XG-CS tablets following the complete formation of PEC on the surface.[73] Li et al confirmed the previous finding when studying the swelling and release behaviour of CS-sodium alginate tablets.[62] It can be noticed from swelling data using 15% LCS (Figure 7b) that a large amount of water was absorbed by the matrix after 1 h dissolution, resulting in a tablet weight increase of > 200 %. However, and following the complete formation of the film on the surface of the tablet, the weight-gain of the swollen tablets levelled off between 2-6 h where the percentage weight gain increased only from ~260 – 420 %, indicating a swelling rate of ~ 40%/h compared to 200%/h for the first hour. A sharp increase in weight gain to around 600% occurred after 8 h (100%/h). From the video images obtained in Figure 10, it can be noted that the developed film started losing its integrity at 8 h and adopted a porous structure rather than the firm and continuous one which occurred between 2-4 h. At 12 h, the film became more porous resulting in full hydration of the tablet and in the disappearance of the dry core region.

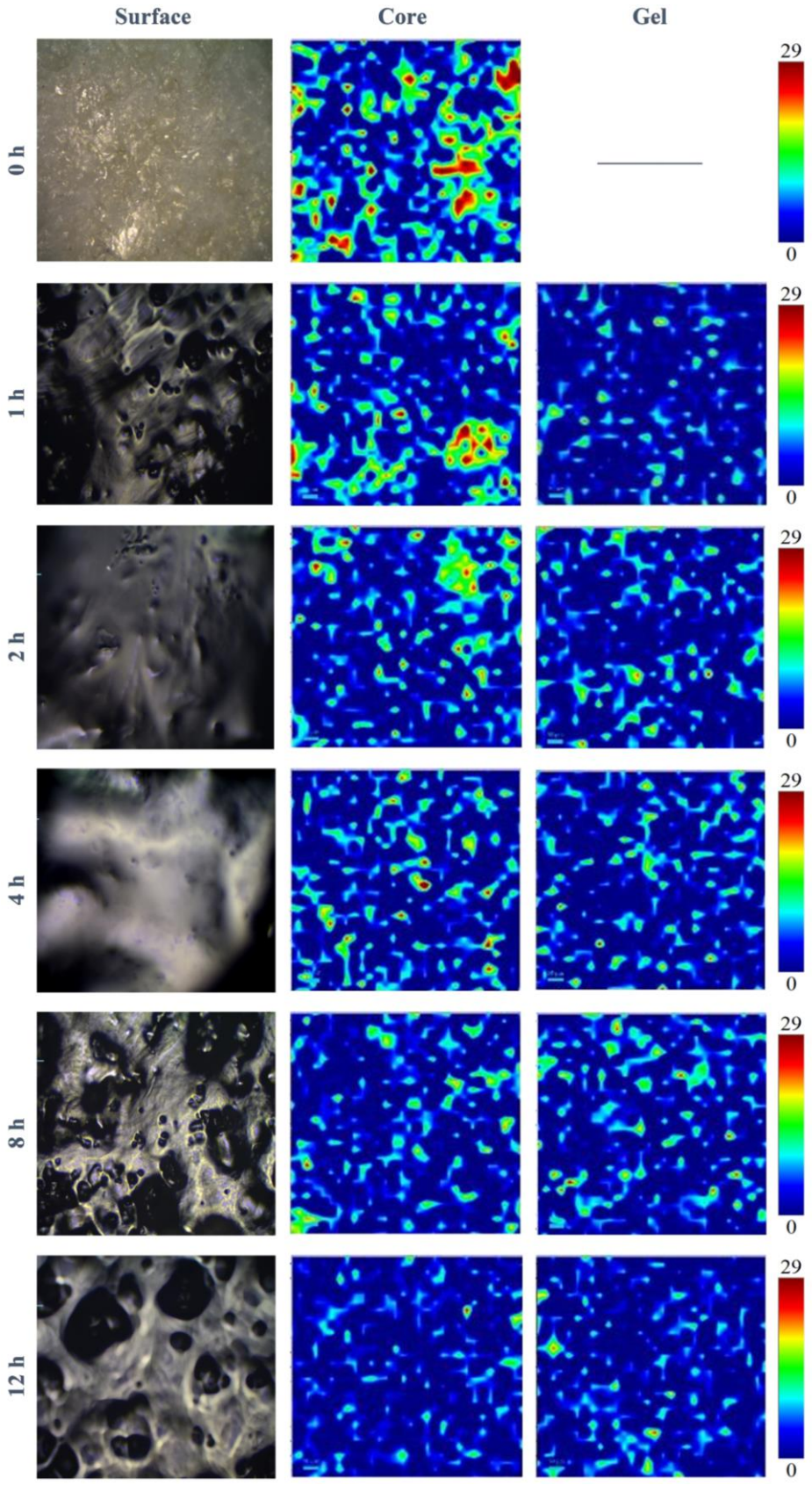

Figure 10 Images on the left side are snapshots obtained from the top surface of the swollen tablets during dissolution (magnification x10). Raman maps, in the mid and right side, show MS distribution between the dry core and the hydrated gel layers of XG-15% LCS tablets as a function of dissolution time. *The area mapped was 720×720 µm^2 using an x10 objective.*

Effect of the pH and ionic strength (μ) of the dissolution media on the release of MS from LCS-XG tablets

Since electrostatic forces are the dominant factor that governs the interaction between LCS and XG, ionization of each polymer will have an influence on PEC formation; as was established in previous work.[50] Therefore, the formulation containing 15% LCS was evaluated at different pH and μ values and then compared to a formulation comprising XG as the sole polymer to assess the effect of adding LCS to the preparation in terms of drug release and matrix swelling. Release of MS from XG based tablets was markedly higher at pH 1.2 than pH 6.8 (Figure 11a, b). This can be explained by the protonation of the free carboxylic groups present in the structure of XG at pH values lower than its pKa (3.1).[74] According to the Henderson-Hasselbalch equation, the concentration of protonated carboxyl groups (-COOH) is ~79 times the unprotonated ($-COO^-$) value at pH 1.2 (Table 7). As a result, the repulsive forces between $-COO^-$ is decreased and XG maintains its ordered helical conformation. Consequently, the drug retardation ability of XG is decreased due to the reduction in water uptake capability. In contrast, the negative charge density of XG is enhanced in acetate and phosphate buffers at pH 4.5 and 6.8, respectively, allowing XG to adopt a disordered coiled conformation. For the 15% LCS preparation, LCS on the tablet surface is fully protonated at pH 1.2, while XG is unionized. Therefore, no electrostatic interactions occurred between LCS and XG and higher drug release rate was noticed. When the pH is increased to 4.5 and 6.8, both XG and LCS become almost fully ionized. Electrostatic attractive forces between the oppositely charged groups of XG and LCS lead to the detected close contact between the two polymers during MD simulations, and the observed low RMSD fluctuation (Figure 2a). As a result, an insoluble PEC is formed on the surface of the tablet. The foregoing assertion is supported by the high positive ΔG_{solv} values (>190 kcal/mol) displayed by the LCS-XG complexes. This indicates unfavourable interactions

of the complexes with aqueous media. In other words, an insoluble and highly stable complex is formed between LCS and XG.

Table 6 Values for the [unprotonated]/[protonated] ratio of LCS and XG in the dissolution media used.

Material	pH 1.2	pH 4.5	pH 6.8
XG	1/79	25/1	5000/1
LCS	0/1	1/63	2/1

The impact of ionic strength of the dissolution media on the swelling behaviour of the two compacts is presented in the data in Figure 11e and f. The high sensitivity of XG to salt concentration in the dissolution medium is clear. A significant decrease in weight gain, around two thirds, was found when the μ value increased from 0 to 0.4 M. Counter-ions cause a reduction in repulsion forces between XG chains. Hence, a rigid helical confirmation stabilized by hydrogen bonds is formed. As a result, a higher fraction of drug is released from the tablets (Figure 11c). MS was fully released after 12 h when the μ = 0.4 M. Calculated f_2 values of new release profiles compared to the original dissolution profile were 55.4, 45.6, and 35.0 when μ = 0.1 M, 0.2 M and 0.4 M, respectively.

Interestingly, incorporating LCS seems to decrease XG sensitivity to minor changes in ionic strength. Tablets comprising 15% LCS displayed an insignificant increase in drug release with elevated μ values of the dissolution media (Figure 11d). A change of no more than 10% in MS release at each time interval was detected. Calculated f_2 values for the dissolution profiles at μ = 0.1, 0.2 and 0.4 M were 68.5, 60.1 and 54.5, respectively, when compared to the dissolution profile of MS from 15% LCS at 0 M. From the average structures of the LCS-XG complexes determined by MDs, it can be noticed that LCS molecules were embedded between the XG chains. Hence, the incorporated LCS molecules shield XG, minimize the interaction of COO^- groups with counter-ions present in the dissolution media, and decrease the susceptibility of the release rate of the drug from XG based tablets on ionic strength.

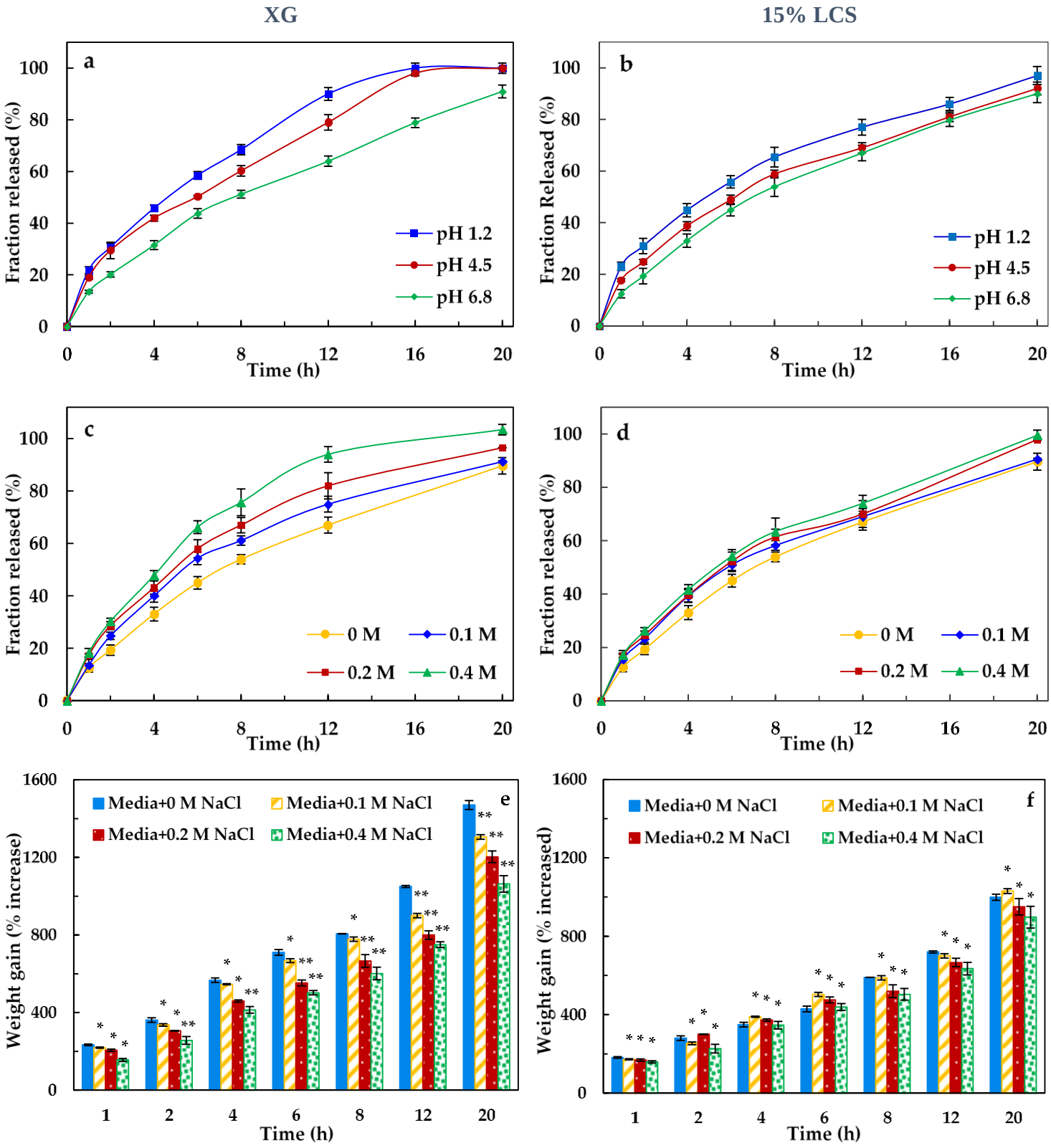

Figure 11 (a-d) The influence of dissolution media pH (at pH 1.2, 4.5 and 6.8) and ionic strength (at μ = 0, 0.1, 0.2 and 0.4 M) on the *in-vitro* release of MS from XG and 15% LCS tablets. *Values represent mean ± SD (n=6).* (e and f) Degree of swelling of XG and 15% LCS formulations from phosphate buffer pH 6.8 at different μ. *Values represent mean ± SD (n=6). (*) denotes insignificant difference in the mean % swelling when μ= 0.1, 0.2 or 0.4 M from the mean % swelling of tablets in 0M dissolution media (p>0.05), whereas (**) denotes a significant difference in the mean (p<0.05)*

A drug release study from tablets comprising XG and 15% HCS was carried out as a comparison with the results obtained from LCS formulation and to assess the performance of the XG-HCS based matrix in controlling the release of MS at different pH and μ values of the dissolution media. Data presented in Figure 12 demonstrates the capability of the matrix to sustain the release of MS. It is obvious that the extent and rate of drug release is highly dependent on the pH and μ of the dissolution media where the drug was fully released after ~ 12 h at low pH (1.2) and high μ (0.2 and 0.4 M) dissolution media. At pH 4.5 and 6.8, the full release of the drug was obtained after 16-20 h. In addition, and when compared to the LCS formulation, a burst release of MS from the formulation can be noticed where around 30% of MS was released in the first two hours (pH 6.8) whereas LCS 15% formulation released < 20% of MS after 2 h of dissolution. These results confirm the finding of MDs which showed that the interaction is more favourable between LCS-XG complexes than HCS-XG. Therefore, more time is needed for HCS to form PEC films on the surface of the tablets; thus, a higher fraction of the drug is dissolved at the beginning of dissolution. Almost similar release profiles of MS were obtained when lowering the pH of the dissolution medium to 4.5. In HCl (pH 1.2), 40% of the incorporated dose was released after 2 h and the drug was fully released (> 85%) after 8 h. Likewise, HCS was not able to overcome the dependency of drug release rate from XG matrixes on the ionic strength of the dissolution media where the fraction of MS released in phosphate buffer solution with added 0.1 M NaCl was 5-10% higher than phosphate buffer alone. A remarkable increase in the cumulative MS released from the XG-HCS matrix was noticed when adding 0.4 M NaCl to the buffer where a 15-25% difference was noticed at each time point when compared to the phosphate buffer. The results obtained are in good agreement with the studies reported in the literature where LCS showed better CR than HCS when combined with XG.[30,39] However, the behaviour and the CR efficiency of the matrices at different pH and μ values of dissolution media was not addressed in the foregoing studies.

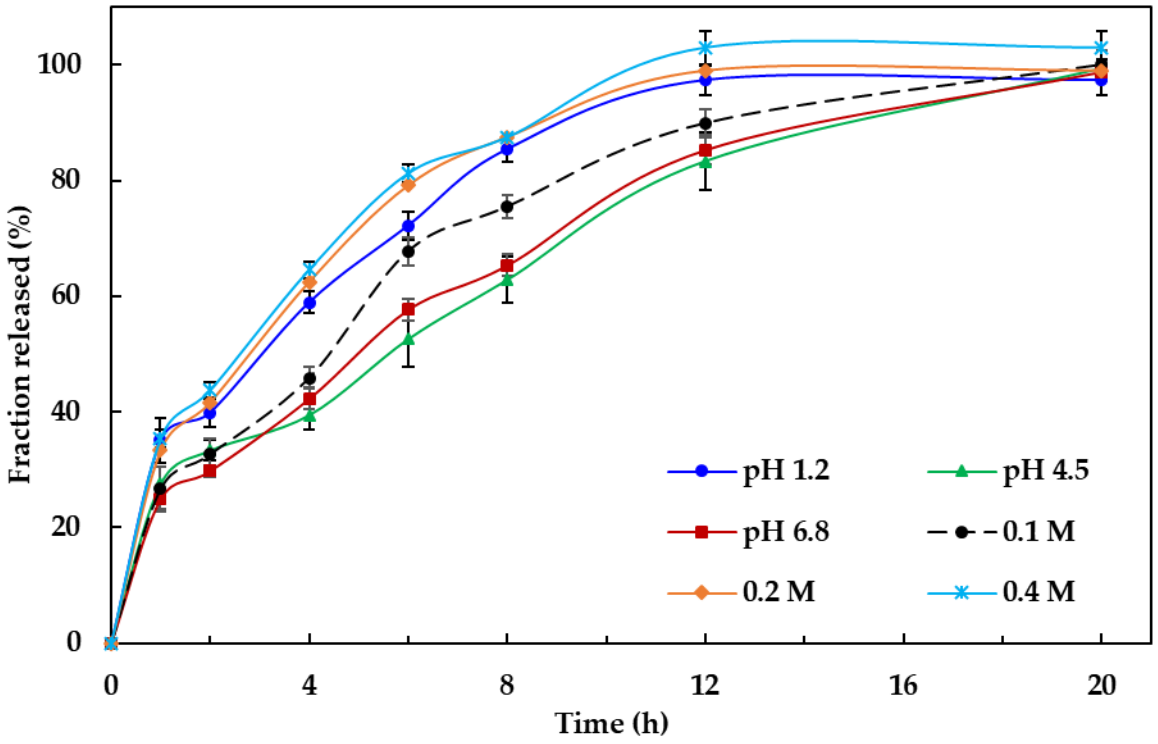

Figure 12 MS release profiles from XG-15% HCS tablets using dissolution media of different pH (1.2, 4.5 and 6.8) and different μ values (0, 0.1, 0.2 and 0.4 M). *Values represent mean ± SD (n=6).*

Dose dumping evaluation

Dose dumping is one of the main drawbacks encountered when using controlled release drug delivery.[75] The solubility of some polymers and other incorporated inactive ingredients might be enhanced in the presence of alcohol. Thus, rapid drug release occurs in the first 1-2 hours which is referred to as (dose dumping).[76] To test the robustness of the prepared formulation, in-vitro release studies for LCS (15%) in an acidic medium (HCl, pH 1.2) were carried out in the presence of ethanol. In the test preparation (LCS 15%), MS showed similar release profiles regardless of ethanol concentration within the dissolution media (Figure 13). On the other hand, dose dumping of MS occurred from the reference formulation (Betaloc ZOK®) when ethanol was introduced to the dissolution medium at concentrations ≥ 20 % (v/v). This can be explained by the hydrophilicity of XG and LCS together with their low solubility in ethanol which resulted in the observed, unaffected drug release. Whereas, the reference formulation contains

a wide range of hydrophobic polymers and inactive ingredients that are highly soluble in ethanol such as, silicon dioxide, ethylcellulose, titanium dioxide, and paraffin. Thus, release of MS from Betaloc ZOK® was enhanced.

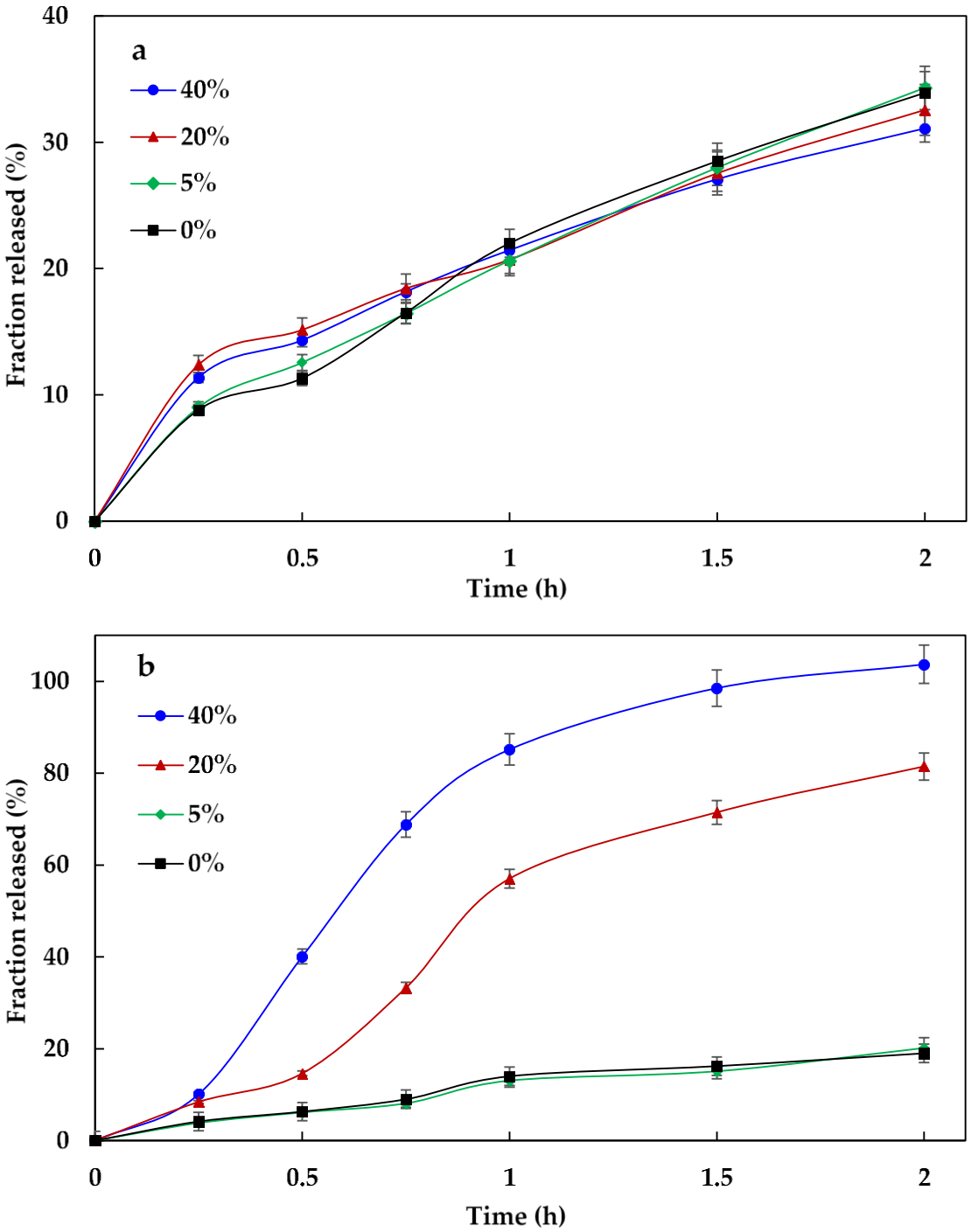

Figure 13 The influence of the presence of ethanol on the *in-vitro* release profile of MS from: (a) 15% LCS tablets and (b) the reference product at 0, 5, 20 and 40% (v/v) ethanol. *Values represent mean ± SD (n=6).*

Conclusions

Computational and drug release studies have demonstrated the superiority of LCS compared to HCS in controlling the release of the entrapped drug when being directly compressed with XG. MDs results suggested that XG forms more stable complexes with LCS compared to HCS. Furthermore, the conformational flexibility of XG chains has been shown to be higher and the time required for LCS-XG complexes to reach equilibrium shorter when LCS was incorporated at low fractions (i.e. 15%). RSM outputs revealed that the major factors determining the rate of MS release from XG-LCS based solid matrices are the P:D ratio and the weight percentage of LCS and that the optimum CR formulation can be obtained by using LCS ≤20%. The developed LCS-XG based tablets showed pH-insensitive CR characteristics when LCS was incorporated at 15% (w/w) using a P:D ratio of 4:1. Moreover, drug release results revealed that the ionic strength of the dissolution media (phosphate buffer) has no impact on tablet swelling and MS release from the 15% LCS matrix system. On the contrary, release profiles of MS from HCS-XG compacts showed high dependency on pH and ionic strength of the dissolution media. Results obtained from Raman mapping and swelling studies for the 15% LCS formulation showed that a self-assembled film was formed on the surface of the tablets due to polyelectrolyte complexation between the two polymers. Upon film formation, a reduction in tablet swelling and drug release was noticed; MS was shown to be more localized in the dry core of the tablets. At this stage, the rate of water penetration into the matrix and polymer relaxation are the main contributors to drug release from the matrix. Thereafter, the formed film started to break down causing the tablets to become fully hydrated and a reduction in the radial swelling of the gel layer occurs resulting in a uniform distribution of the drug within the matrix. The rate of drug diffusion through the hydrated tablet together with the rate of matrix erosion are suggested to govern the rate of drug release at this stage of dissolution.

The study reported herein addresses the utility of computational tools in predicting and minimizing the experimental work required to design and optimize drug delivery systems. In addition, it establishes the strong possibility of using a CR dosage form based on two biopolymers that is ready for large scale production using an accessible, cost-effective, and "simple" methodology. Further investigations toward the applicability of this system to a wide range of APIs, and on its capability to be used as a universal CR system are currently under investigation by the authors of this study.

AUTHOR INFORMATION

Corresponding author

Email: dr.badwan@jpm.com.jo

ORCID: httpS://orcid.org/0000-0003-1018-6358

ORCID for co-authors

Suha Dadou: https://orcid.org/0000-0002-2770-7677

AUTHOR CONTRIBUTIONS

All the authors contributed to experimental design and planning. Experimental studies were undertaken by S.M.D; computational studies were performed by S.M.D and M.I.E-B. All the authors contributed to the writing of the manuscript.

COMPETING INTERESTS

The authors declare no competing financial interests.

CHEMICAL COMPOUNDS STUDIED IN THIS ARTICLE

Chitosan (PubChem CID: 21896651)

Xanthan gum (PubChem CID: 7107)

Metoprolol succinate (PubChem CID: 62937)

ABBREVIATIONS

APIs active pharmaceutical ingredients

CR controlled-release

CS chitosan

D drug

HCS high molecular weight chitosan

LCS low molecular weight chitosan

MDs molecular dynamics simulation

MM-PBSA Molecular Mechanics-Poisson–Boltzmann surface area

MS metoprolol succinate

P polymer

Rg radius of gyration

RSM response surface method

XG xanthan gum

REFERENCES

(1) Siegel, R. A.; Rathbone, M. J. Overview of Controlled Release Mechanisms. In *Fundamentals and Applications of Controlled Release Drug Delivery.*; Springer: Boston, MA, 2012; pp 19–43.

(2) Hoffman, A. S. The Origins and Evolution of "Controlled" Drug Delivery Systems. *J. Control. Release* **2008**, *132* (3), 153–163.

(3) Pundir, S.; Badola, A.; Sharma, D. Sustained Release Matrix Technology and Recent Advance in Matrix Drug Delivery System: A Review. *Int. J. Drug Res. Technol.* **2013**, *3* (1), 12–20.

(4) Nokhodchi, A.; Raja, S.; Patel, P.; Asare-Addo, K. The Role of Oral Controlled Release Matrix Tablets in Drug Delivery Systems. *Bioimpacts* **2012**, *2* (4), 175–187.

(5) Dadou, S. M.; Antonijevic, M. D.; Chowdhry, B. Z.; Badwan, A. A. An Overview of Chitosan-Xanthan Gum Matrices as Controlled Release Drug Carriers. In *Chitin-Chitosan - Myriad Functionalities in Science and Technology*; Dongre, R., Ed.; IntechOpen, 2018; pp 220–243.

(6) Lee, P. I.; Li, J. X. Evolution of Oral Controlled Release Dosage Forms. In *Oral Controlled*

Release Formulation Design and Drug Delivery: Theory to Practice; Wen, H., Park, K., Eds.; John Wiley & Sons, Inc., 2010; pp 21–31.

(7) Malafaya, P. B.; Silva, G. A.; Reis, R. L. Natural-Origin Polymers as Carriers and Scaffolds for Biomolecules and Cell Delivery in Tissue Engineering Applications. *Adv. Drug Deliv. Rev.* **2007**, *59* (4–5), 207–233.

(8) Racoviţă, Ş.; Vasiliu, S.; Popa, M.; Luca, C. Polysaccharides Based on Micro- and Nanoparticles Obtained by Ionic Gelation and Their Applications as Drug Delivery Systems. *Rev. Roum. Chim.* **2009**, *54* (9), 709–718.

(9) Alvarez-Lorenzo, C.; Blanco-Fernandez, B.; Puga, A. M.; Concheiro, A. Crosslinked Ionic Polysaccharides for Stimuli-Sensitive Drug Delivery. *Adv. Drug Deliv. Rev.* **2013**, *65* (9), 1148–1171.

(10) Talukdar, M. M.; Plaizier-Vercammen, J. Evaluation of Xanthan Cum as a Hydrophilic Matrix for Controlled-Release Dosage Form Preparations. *Drug Dev. Ind. Pharm.* **1993**, *19* (9), 1037–1046.

(11) Benny, I. S.; Gunasekar, V.; Ponnusami, V. Review on Application of Xanthan Gum in Drug Delivery. *Int. J. PharmTech Res.* **2014**, *6* (4), 1322–1326.

(12) Salyers, A. A.; Vercellotti, J. R.; West, S. E.; Wilkins, T. D. Fermentation of Mucin and Plant Polysaccharides by Strains of Bacteroides from the Human Colon. *Appl. Environ. Microbiol.* **1977**, *33* (2), 319–322.

(13) Lu, M. F.; Woodward, L.; Borodkin, S. Xanthan Gum and Alginate Based Controlled Release Theophylline Formulations. *Drug Dev. Ind. Pharm.* **1991**, *17* (14), 1987–2004.

(14) Talukdar, M. M.; Kinget, R. Swelling and Drug Release Behaviour of Xanthan Gum Matrix Tablets. *Int. J. Pharm.* **1995**, *120* (1), 63–72.

(15) Santos, H.; Veiga, F.; Pina, M. E.; Sousa, J. J. Compaction, Compression and Drug Release Properties of Diclofenac Sodium and Ibuprofen Pellets Comprising Xanthan Gum as a Sustained Release Agent. *Int. J. Pharm.* **2005**, *295* (1–2), 15–27.

(16) García-Ochoa, F.; Santos, V. E.; Casas, J. A.; Gómez, E. Xanthan Gum: Production, Recovery, and Properties. *Biotechnol. Adv.* **2000**, *18* (7), 549–579.

(17) Faria, S.; De Oliveira Petkowicz, C. L.; De Morais, S. A. L.; Terrones, M. G. H.; De Resende, M. M.; De Frana, F. P.; Cardoso, V. L. Characterization of Xanthan Gum Produced from Sugar Cane Broth. *Carbohydr. Polym.* **2011**, *86* (2), 469–476.

(18) Petri, D. F. S. Xanthan Gum: A Versatile Biopolymer for Biomedical and Technological Applications. *J. Appl. Polym. Sci.* **2015**, *132* (23), 42035.

(19) Bueno, V. B.; Bentini, R.; Catalani, L. H.; Petri, D. F. S. Synthesis and Swelling Behavior of Xanthan-Based Hydrogels. *Carbohydr. Polym.* **2013**, *92* (2), 1091–1099.

(20) Fukuda, M.; Peppas, N. A.; McGinity, J. W. Properties of Sustained Release Hot-Melt Extruded Tablets Containing Chitosan and Xanthan Gum. *Int. J. Pharm.* **2006**, *310* (1–2), 90–100.

(21) Andreopoulos, A. G.; Tarantili, P. A. Xanthan Gum as a Carrier for Controlled Release of Drugs. *J. Biomater. Appl.* **2001**, *16* (1), 34–46.

(22) Paradossi, G.; Chiessi, E.; Barbiroli, A.; Fessas, D. Xanthan and Glucomannan Mixtures: Synergistic Interactions and Gelation. *Biomacromolecules* **2002**, *3* (3), 498–504.

(23) Baichwal, A. R.; Staniforth, J. N. Sustained Release Excipient and Tablet Formulation. U.S. Patent. No. 5,128,143, 1992.

(24) Staniforth, J. N.; Baichwal, A. R. TIMERx: Novel Polysaccharide Composites for Controlled/Programmed Release of Drugs in the Gastrointestinal Tract. *Expert Opin. Drug Deliv.* **2005**, *2* (3), 587–595.

(25) Wu, Q.; Therriault, D.; Heuzey, M. C. Processing and Properties of Chitosan Inks for 3D Printing of Hydrogel Microstructures. *ACS Biomater. Sci. Eng.* **2018**, *4* (7), 2643–2652.

(26) Badwan, A. A.; Al-Remawi, M.; Salem, M. Universal Controlled-Release Composition Comprising Chitosan. European Patent. EP1512394, 2008.

(27) Luo, Y.; Wang, Q. Recent Development of Chitosan-Based Polyelectrolyte Complexes with Natural Polysaccharides for Drug Delivery. *Int. J. Biol. Macromol.* **2014**, *64*, 353–367.

(28) Corti, G.; Cirri, M.; Maestrelli, F.; Mennini, N.; Mura, P. Sustained-Release Matrix Tablets of Metformin Hydrochloride in Combination with Triacetyl-β-Cyclodextrin. *Eur. J. Pharm. Biopharm.* **2008**, *68* (2), 303–309.

(29) Eftaiha, A. F.; Qinna, N.; Rashid, I. S.; Al Remawi, M. M.; Al Shami, M. R.; Arafat, T. A.; Badwan, A. A. Bioadhesive Controlled Metronidazole Release Matrix Based on Chitosan and Xanthan Gum. *Mar. Drugs* **2010**, *8* (5), 1716–1730.

(30) Al-Akayleh, F.; Al Remawi, M.; Rashid, I.; Badwan, A. Formulation and In Vitro Assessment of Sustained Release Terbutaline Sulfate Tablet Made from Binary Hydrophilic Polymer Mixtures. *Pharm. Dev. Technol.* **2013**, *18* (5), 1204–1212.

(31) Al Remawi, M.; Al-Akayleh, F.; Salem, M. S.; Al Shami, M.; Badwan, A. Application of an Excipient Made from Chitosan and Xanthan Gum as a Single Component for the Controlled Release of Ambroxol. *J. Excipients Food Chem.* **2013**, *4* (2), 48–57.

(32) Al-Akayleh, F.; Al Remawi, M.; Salem, M. S.; Badwan, A. Using Chitosan and Xanthan Gum Mixtures as Excipients in Controlled Release Formulations of Ambroxol HCl - in Vitro Drug Release and Swelling Behavior. *J. Excipients Food Chem.* **2014**, *5* (2), 140–148.

(33) Sinha, V. R.; Kumria, R. Polysaccharides in Colon-Specific Drug Delivery. *Int. J. Pharm.* **2001**, *224* (1–2), 19–38.

(34) Abdul Rahim, S. A.; Elkordy, A. A. Application of Xanthan Gum as a Sustained Release Agent. In *Xanthan Gum: Applications and Research Studies*; Nova Science Publishers, Inc.: New York, 2016; pp 67–96.

(35) Huang, G.; Liu, Y.; Chen, L. Chitosan and Its Derivatives as Vehicles for Drug Delivery. *Drug Deliv.* **2017**, *24* (2), 108–113.

(36) M.Ways, T. M.; Lau, W. M.; Khutoryanskiy, V. V. Chitosan and Its Derivatives for Application in Mucoadhesive Drug Delivery Systems. *Polymers.* **2018**, *10* (3), 267.

(37) Tan, W.; Li, Q.; Dong, F.; Zhang, J.; Luan, F.; Wei, L.; Chen, Y.; Guo, Z. Novel Cationic Chitosan Derivative Bearing 1,2,3-Triazolium and Pyridinium: Synthesis, Characterization, and Antifungal Property. *Carbohydr. Polym.* **2018**, *182*, 180–187.

(38) Dumitriu, S.; Chornet, E.; Vidal, P. Polyionic Insoluble Hydrogels Comprising Xanthan and Chitosan. U.S. Patent No. 5,620,706, 1997.

(39) Alakayleh, F.; Rashid, I.; Al-Omari, M. M.; Al-Sou'od, K.; Chowdhry, B. Z.; Badwan, A. A. Compression Profiles of Different Molecular Weight Chitosans. *Powder Technol.* **2016**, *299*, 107–118.

(40) Lexicomp Online. Metoprolol: Drug information. Hudson, Ohio, Wolters Kluwer Clinical Drug Information Inc. 2016, https://online.lexi.com/ (accessed Sep 12, 2017).

(41) Wishart, D. S.; Feunang, Y. D.; Guo, A. C.; Lo, E. J.; Marcu, A.; Grant, J. R.; Sajed, T.; Johnson, D.; Li, C.; Sayeeda, Z.; Assempour, N; Iynkkaran, I; Liu, Y; Maciejewski, A; Gale, N; Wilson, A; Chin, L; Cummings, R; Le, D; Pon, A; Knox, C; Wilson, M. DrugBank 5.0: A Major Update to the DrugBank Database for 2018. *Nucleic Acids Res.* **2017**, *46* (D1), D1074–D1082.

(42) Kirschner, K. N.; Yongye, A. B.; Tschampel, S. M.; González-Outeiriño, J.; Daniels, C. R.; Foley, B. L.; Woods, R. J. GLYCAM06: A Generalizable Biomolecular Force Field. Carbohydrates. *J. Comput. Chem.* **2008**, *29* (4), 622–655.

(43) Case, D. A.; Darden, T. A.; Cheatham, T. E.; Simmerling, C. L.; Wang, J.; Duke, R. E.; Luo, R.; Walker, R. C.; Zhang, W.; Merz, K. M.; Roberts, B.; Wang, B.; Hayik, S.; Roitberg, A.; Seabra, G.; Kolossváry, I.; Wong, K.F.; Paesani, F.; Vanicek, J.; Liu, J.; Wu, X.; Brozell, S.R.; Steinbrecher, T.; Gohlke, H.; Cai, Q.; Ye, X.; Wang, J.; Hsieh, M.-J.; Cui, G.; Roe, D.R.; Mathews, D.H.; Seetin, M.G.; Sagui, C.; Babin, V.; Luchko, T.; Gusarov, S.; Kovalenko, A.; Kollman, P.A. (2010), AMBER 11, *University of California, San Francisco*.

(44) Carbohydrate Builder. Woods Group, (2005-2017), GLYCAM web, Complex Carbohydrate Research Center, University of Georgia, Athens, GA. http://glycam.org (accessed May 20, 2017).

(45) Darden, T.; York, D.; Pedersen, L. Particle Mesh Ewald: An N ·log(N) Method for Ewald Sums in Large Systems. *J. Chem. Phys.* **1993**, *98* (12), 10089–10092.

(46) Humphrey, W.; Dalke, A.; Schulten, K. VMD: Visual Molecular Dynamics. *J. Mol. Graph.* **1996**, *14* (1), 33–38.

(47) Honig, B.; Nicholls, A. Classical Electrostatics in Biology and Chemistry. *Science.* **1995**, *268* (5214), 1144–1149.

(48) ICH Harmonised Tripartite Guideline. Validation of analytical procedures: text and methodology Q2 (R1), International Council for Harmonisation of Technical Requirements for Pharmaceuticals for Human Use, 2005. https://www.ich.org/products/guidelines.html (accessed Nov 23, 2017).

(49) Food and Drug Administration (FDA). Draft Guidance on Metoprolol Succinate, 2008. https://www.fda.gov/downloads/Drugs/.../Guidances/UCM088687.pdf (accessed Jan 14, 2018).

(50) Dadou, S. M.; El-Barghouthi, M. I.; Alabdallah, S. K.; Badwan, A. A.; Antonijevic, M. D.; Chowdhry, B. Z. Effect of Protonation State and N-Acetylation of Chitosan on Its Interaction with Xanthan Gum: A Molecular Dynamics Simulation Study. *Mar. Drugs* **2017**, *15* (10), 298–317.

(51) Moradi, S.; Hosseini, E.; Abdoli, M.; Khani, S.; Shahlaei, M. Comparative Molecular Dynamic Simulation Study on the Use of Chitosan for Temperature Stabilization of Interferon AII. *Carbohydr. Polym.* **2019**, *203*, 52–59.

(52) Li, J.; Du, Y.; Liang, H. Low Molecular Weight Water-Soluble Chitosans: Preparation with the Aid of Cellulase, Characterization, and Solubility. *J. Appl. Polym. Sci.* **2006**, *102* (2), 1098–1105.

(53) Kubota, N.; Tatsumoto, N.; Sano, T.; Toya, K. A Simple Preparation of Half N-Acetylated Chitosan Highly Soluble in Water and Aqueous Organic Solvents. *Carbohydr. Res.* **2000**, *324* (4), 268–274.

(54) Malakar, J.; Nayak, A. K.; Goswami, S. Use of Response Surface Methodology in the Formulation and Optimization of Bisoprolol Fumarate Matrix Tablets for Sustained Drug Release. *ISRN Pharm.* **2012**, *2012*, 1–10.

(55) Mundada, P. K.; Sawant, K. K.; Mundada, V. P. Formulation and Optimization of Controlled Release Powder for Reconstitution for Metoprolol Succinate Multi Unit Particulate Formulation Using Risk Based QbD Approach. *J. Drug Deliv. Sci. Technol.* **2017**, *41*, 462–474.

(56) Gohel, M. C.; Parikh, R. K.; Nagori, S. a; Jena, D. G. Fabrication of Modified Release Tablet Formulation of Metoprolol Succinate Using Hydroxypropyl Methylcellulose and Xanthan Gum. *AAPS PharmSciTech* **2009**, *10* (1), 62–68.

(57) Sahu, S. K.; Sharma, A. K. Influence of Carbopol and Polyox on the Release of Metoprolol Succinate From Extended-Release Matrix Tablets: A Doe Approach and in-Vivo Evaluation. *World J. Pharm. Pharm. Sci.* **2018**, *7* (4), 1228–1239.

(58) Ghori, M. U.; Conway, B. R. Hydrophilic Matrices for Oral Control Drug Delivery. *Am. J. Pharmacol. Sci.* **2015**, *3* (5), 103–109.

(59) Varshosaz, J.; Tavakoli, N.; Eram, S. A. Use of Natural Gums and Cellulose Derivatives in Production of Sustained Release Metoprolol Tablets. *Drug Deliv. J. Deliv. Target. Ther. Agents* **2006**, *13* (2), 113–119.

(60) Ritthidej, G. C.; Chomto, P.; Pummangura, S.; Menasveta, P. Chitin and Chitosan as Disintegrants in Paracetamol Tablets. *Drug Dev. Ind. Pharm.* **1994**, *20* (13), 2109–2134.

(61) Food and Drug Administration (FDA). Guidance for Industry: SUPAC-MR: Modified Release Solid Oral Dosage Forms; Scale-Up and Post-Approval Changes: Chemistry, Manufacturing and Controls."Vitro Dissolution Testing, and In Vivo Bioequivalence Documentation". *Rockville, USA*. 1997.

(62) Li, L.; Wang, L.; Shao, Y.; Ni, R.; Zhang, T.; Mao, S. Drug Release Characteristics from Chitosan-Alginate Matrix Tablets Based on the Theory of Self-Assembled Film. *Int. J. Pharm.* **2013**, *450* (1–2), 197–207.

(63) Salamanca, C. H.; Yarce, C. J.; Moreno, R. A.; Prieto, V.; Recalde, J. Natural Gum-Type Biopolymers as Potential Modified Nonpolar Drug Release Systems. *Carbohydr. Polym.* **2018**, *189*, 31–38.

(64) Li, L.; Wang, L.; Li, J.; Jiang, S.; Wang, Y.; Zhang, X.; Ding, J.; Yu, T.; Mao, S. Insights into the Mechanisms of Chitosan-Anionic Polymers-Based Matrix Tablets for Extended Drug Release. *Int. J. Pharm.* **2014**, *476* (1), 253–265.

(65) Venkateswrlu, P. Remote Sensing and GIS to Combat Drought Disaster : An Indian Example. *Int. Geosci. Remote Sens. Symp.* **2004**, *4*, 2294–2297.

(66) Mylangam, C. K.; Beeravelli, S.; Medikonda, J.; Pidaparthi, J. S.; Kolapalli, V. R. M. Badam Gum: A Natural Polymer in Mucoadhesive Drug Delivery. Design, Optimization, and Biopharmaceutical Evaluation of Badam Gum-Based Metoprolol Succinate Buccoadhesive Tablets. *Drug Deliv.* **2016**, *23* (1), 195–206.

(67) Ewing, A. V.; Kazarian, S. G. Recent Advances in the Applications of Vibrational Spectroscopic Imaging and Mapping to Pharmaceutical Formulations. *Spectrochim. Acta - Part A Mol. Biomol. Spectrosc.* **2018**, *197*, 10–29.

(68) Xiao, L.; Schultz, Z. D. Spectroscopic Imaging at the Nanoscale: Technologies and Recent Applications. *Anal. Chem.* **2018**, *90* (1), 440–458.

(69) Eksi-Kocak, H.; Ilbasmis Tamer, S.; Yilmaz, S.; Eryilmaz, M.; Boyaci, I. H.; Tamer, U. Quantification and Spatial Distribution of Salicylic Acid in Film Tablets Using FT-Raman Mapping with Multivariate Curve Resolution. *Asian J. Pharm. Sci.* **2018**, *13* (2), 155–162.

(70) Gordon, K. C.; McGoverin, C. M. Raman Mapping of Pharmaceuticals. *Int. J. Pharm.* **2011**,

417 (1–2), 151–162.

(71) Wray, P. S.; Sinclair, W. E.; Jones, J. W.; Clarke, G. S.; Both, D. The Use of in Situ near Infrared Imaging and Raman Mapping to Study the Disproportionation of a Drug HCl Salt during Dissolution. *Int. J. Pharm.* **2015**, *493* (1–2), 198–207.

(72) Phaechamud, T.; Ritthidej, G. C. Sustained-Release from Layered Matrix System Comprising Chitosan and Xanthan Gum. *Drug Dev. Ind. Pharm.* **2007**, *33* (6), 595–605.

(73) Shao, Y.; Li, L.; Gu, X.; Wang, L.; Mao, S. Evaluation of Chitosan-Anionic Polymers Based Tablets for Extended-Release of Highly Water-Soluble Drugs. *Asian J. Pharm. Sci.* **2015**, *10* (1), 24–30.

(74) Mikac, U.; Sepe, A.; Baumgartner, S.; Kristl, J. The Influence of High Drug Loading in Xanthan Tablets and Media with Different Physiological PH and Ionic Strength on Swelling and Release. *Mol. Pharm.* **2016**, *13* (3), 1147–1157.

(75) Jedinger, N.; Khinast, J.; Roblegg, E. The Design of Controlled-Release Formulations Resistant to Alcohol-Induced Dose Dumping - A Review. *Eur. J. Pharm. Biopharm.* **2014**, *87* (2), 217–226.

(76) Gujjar, C. Y.; Rallabandi, B. C.; Gannu, R.; Deulkar, V. S. Development and Optimization of a Novel Prolonged Release Formulation to Resist Alcohol-Induced Dose Dumping. *AAPS PharmSciTech* **2016**, *17* (2), 350–357.

Table of Contents Use Only

Elucidation of the Controlled Release Behavior of Metoprolol Succinate from Directly Compressed Xanthan Gum-Chitosan Polymers: Computational and Experimental Studies

Suha M. Dadou, Musa I. El-Barghouthi, Milan D. Antonijevic, Babur Z. Chowdhry, and Adnan A. Badwan